Single-Crystal Interference Coatings for Laser-Based Metrology and Manufacturing Systems

Presented by:

OSA Thin Films Technical Group

Thin Films Technical Group Leadership Team

https://www.osa.org/ThinFilmsTG

Chair
Dr. Jue Wang
Corning Incorporated USA
wangj3@corning.com

Vice Chair
Dr. Anna Sytchkova
ENEA - Casaccia Research Centre, Italy
anna.sytchkova@enea.it

Social Media Officer
Dr. Selim Elhadj
Lawrence Livermore National Laboratory, USA
elhadj2@llnl.gov

Event Officer
Dr. Xinbin Cheng
Tongji University, China
chengxb@tongji.edu.cn

Webinar Officer
(Nano-Structured Based)
Dr. Amirkianoosh (Kiano) Kiani
UOIT, Canada
Amirkianoosh.kiani@uoit.ca

Webinar Officer
(PVD Based)
Dr. Julien Lumeau
Institut Fresnel, France
julien.lumeau@fresnel.fr

Webinar Officer
(ALD Based)
Dr. Adriana Szeghalmi
Fraunhofer IOF, Germany
Adriana.Szeghalmi@iof.fraunhofer.de

Thin Films Technical Group at a Glance

- Focus
  - Optical thin films from fundamentals to applications
  - Our group serves over 1000 global members
- Mission
  - Connect people from academia, institutions and industries in the field
  - Bridge the fundamentals, the know-hows and the new developments
  - Promote networking and career development through continuous learning
- Find Us Here
  - OSA Technical Group Website: www.osa.org/ThinFilmsTG
  - LinkedIn: www.linkedin.com/groups/4783616

Interested in presenting your research?
Have ideas for our group activities/events?
Please contact us. Thank you!

Events of Thin Films Technical Group in 2019

- ***Optical Monitoring Systems for Optical Coatings***
  12 February 2019 by Dr. Binyamin Robin

- ***Quality Control and Thin Film Metrology for Future Optical Components***
  14 May 2019 by Dr. Lars Jensen

- **Meet and Greet at OIC 2019**
  6 June 2019 by Dr. Jue Wang

- ***High reflectance/transmittance measurements of laser optics with cavity ring-down (CRD) technique***
  24 September 2019 8:30 AM ~ 9:30 AM EDT
  by Prof. Bincheng Li

- ***Substrate-Transferable Single-Crystal Optical Coatings***
  5 November 2019 9:30 AM ~ 10:30 AM EST by Dr. Garrett Cole

You may find information on upcoming webinars and access the past presentations via on-demand webinars at
https://www.osa.org/en-us/get_involved/technical_groups/technical_group_webinars/#ondemand

Today’s Webinar

Single-crystal interference coatings for laser-based metrology and manufacturing systems
By Garrett D. Cole

Garrett D. Cole is Co-Founder of Crystalline Mirror Solutions. He obtained his PhD in Materials from UC Santa Barbara in 2005. Since completing his doctorate, he has held different positions in academia and industry.

Dr. Cole has co-authored 2 book chapters and published more than 50 journal articles and conference proceedings in high impact factor journals.

He is an expert in micro- and nanofabrication, tunable semiconductor lasers, and cavity optomechanics

CMS
CRYSTALLINE MIRROR SOLUTIONS

Single-crystal interference coatings for laser-based metrology and manufacturing systems

November 5, 2019

- **Introduction to substrate-transferred crystalline coatings**
- **Microfabrication-based coating process overview**
- **Advantages of bonded single-crystal interference coatings**
  - **low elastic losses and minimal Brownian noise**
  - **mid-infrared optical transparency**
  - **high thermal conductivity**

CMS

	Technology	Technical challenge	Solution
Time	Optical clocks 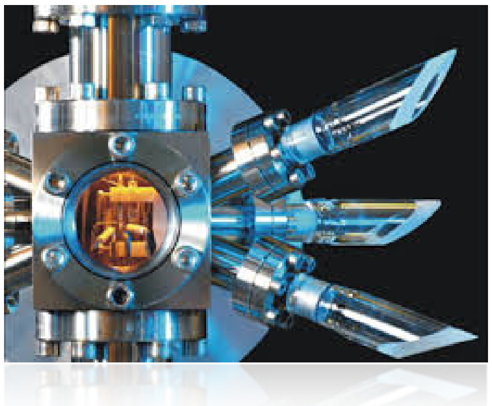	• Clock uncertainty & stability **limited by thermal noise**	**Low-noise coatings will enable the world's most stable lasers**
Space	Gravitational wave detectors 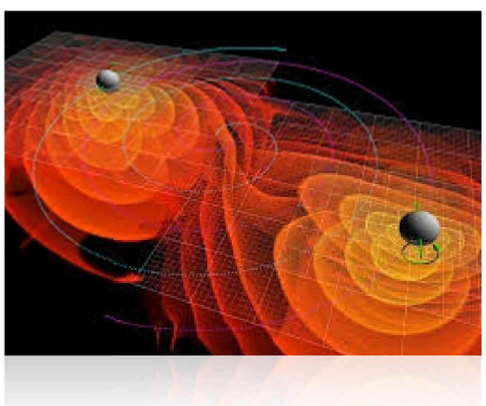	• Coating **Brownian noise** largely limits strain sensitivity	**Low-noise coatings will expand the viewable universe**

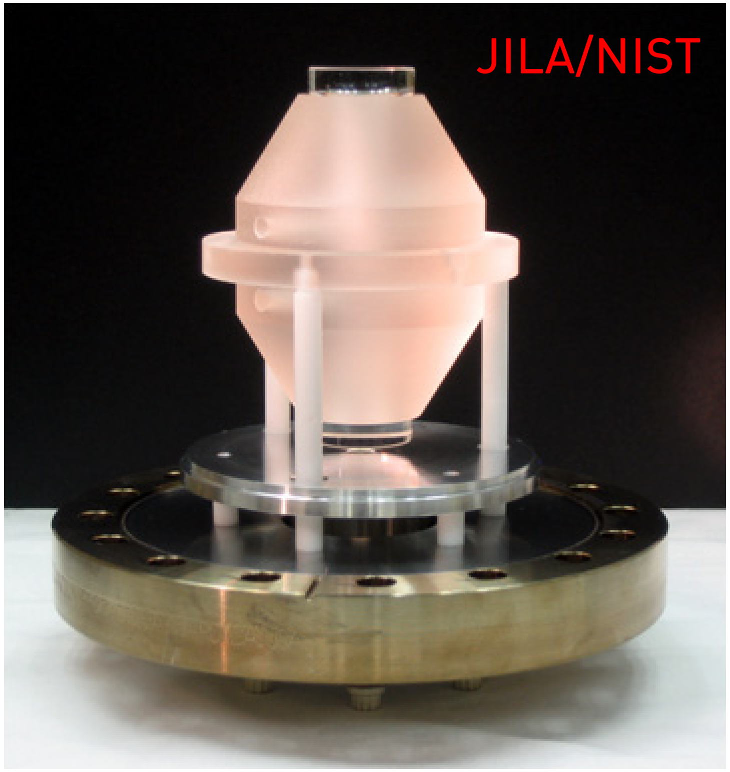

- Precision interferometers are now limited by Brownian noise
  - from cm-scale reference cavities to km-length GW detectors

Brownian Noise Consequences

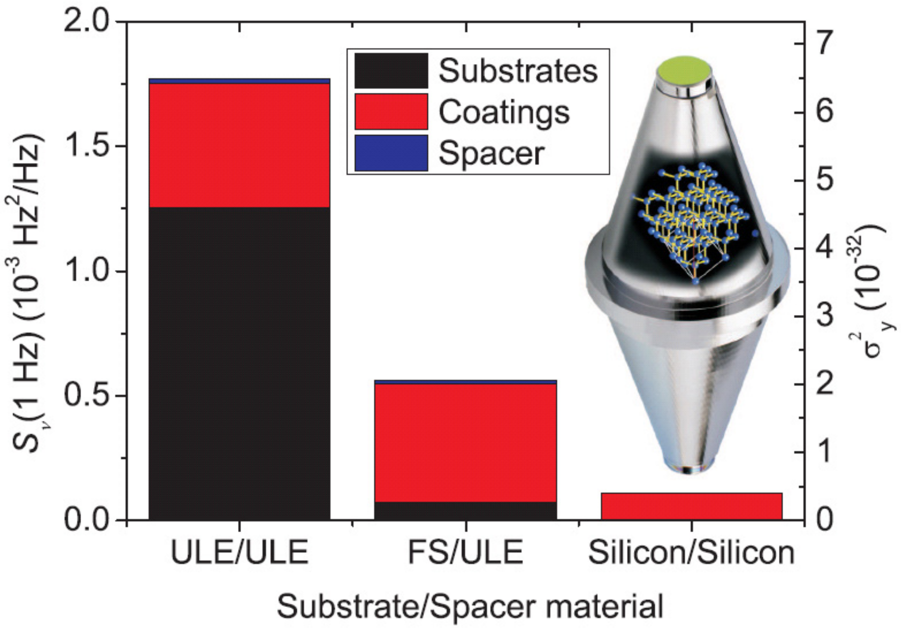

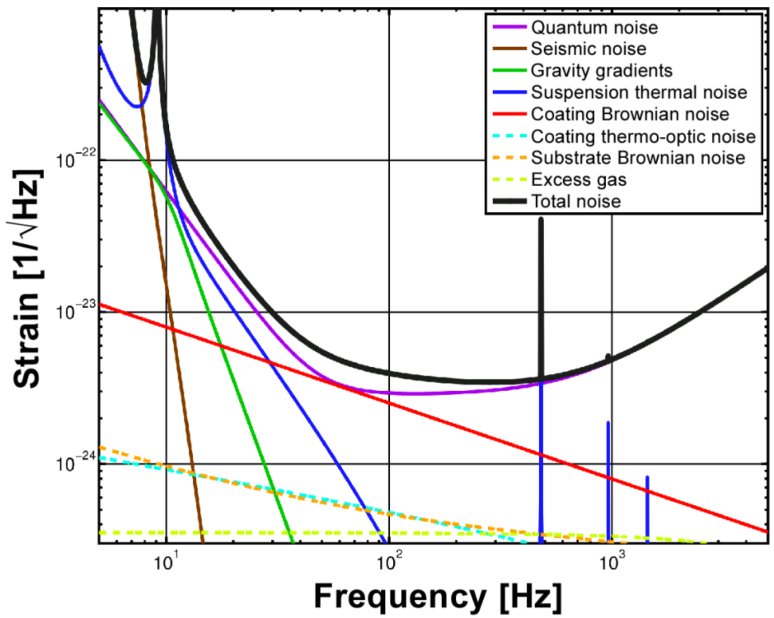

- IBS-deposited optical coatings (Ta_2O_5/SiO_2) are now a key limitation
  - from LSC studies by Crooks, Harry, Penn, etc. Ta_2O_5 is the culprit
  - loss angle has been reduced by a factor of ~2 over the last decade
- Alternative interference coatings are now being explored
  - goal: simultaneous achievement of high optical and mechanical quality

Kessler, et al. Nature Photonics 2012 | Harry, Bodiya, DeSalvo eds., Cambridge Univ. Press 2012

Timeline of Competing Coating Technologies

Current amorphous coatings

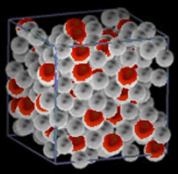

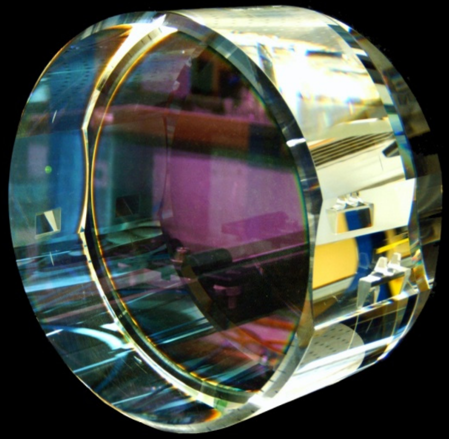

1857	1907	1935	1979
Arc Evaporation	E-beam Evaporation	Magnetron Sputtering	Ion-beam Sputtering

Timeline of Competing Coating Technologies

Fluctuating mirror

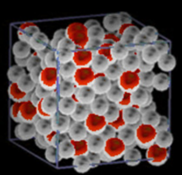

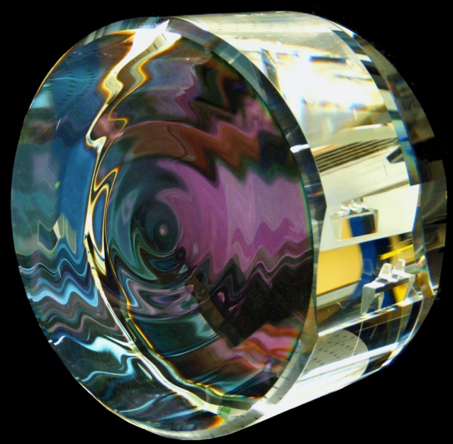

1857
Arc
Evaporation

1907
E-beam
Evaporation

1935
Magnetron
Sputtering

1979
Ion-beam
Sputtering

Timeline of Competing Coating Technologies

Current amorphous coatings

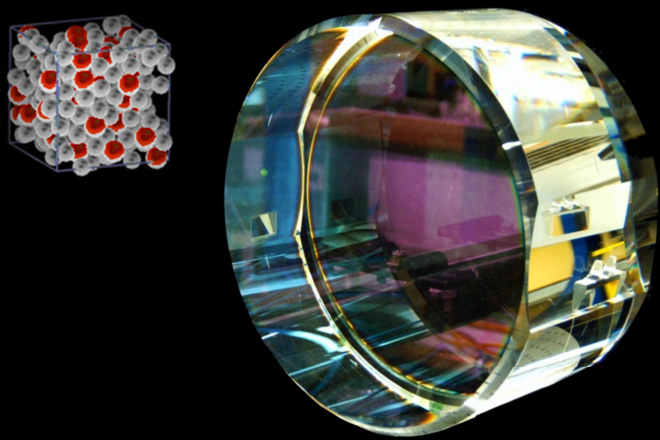

Semiconductor Supermirrors

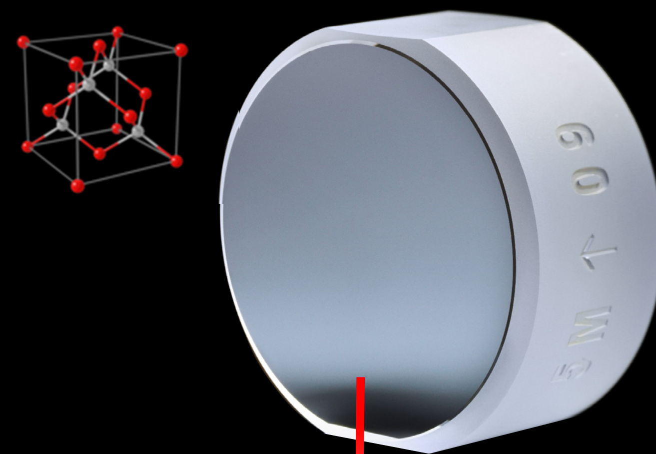

2012
Crystalline Coatings

1857
Arc
Evaporation

1907
E-beam
Evaporation

1935
Magnetron
Sputtering

1979
Ion-beam
Sputtering

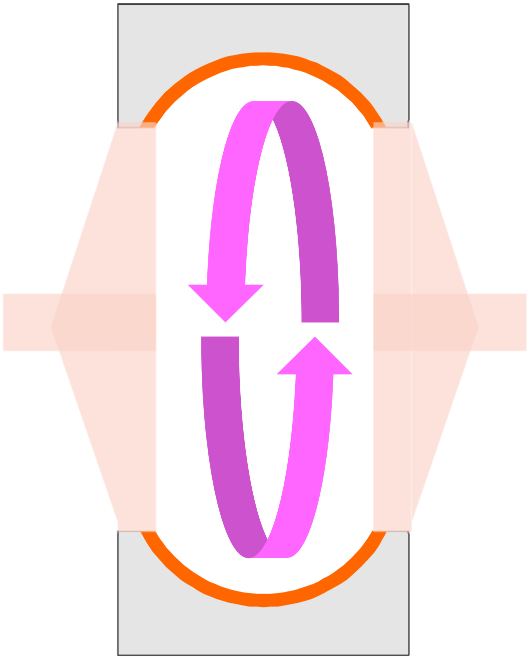

- Damping leads to length perturbation: fluctuation-dissipation theorem
  - off-resonant Brownian noise scales with mechanical loss in system
  - Brownian noise minimized via low-mechanical-loss materials

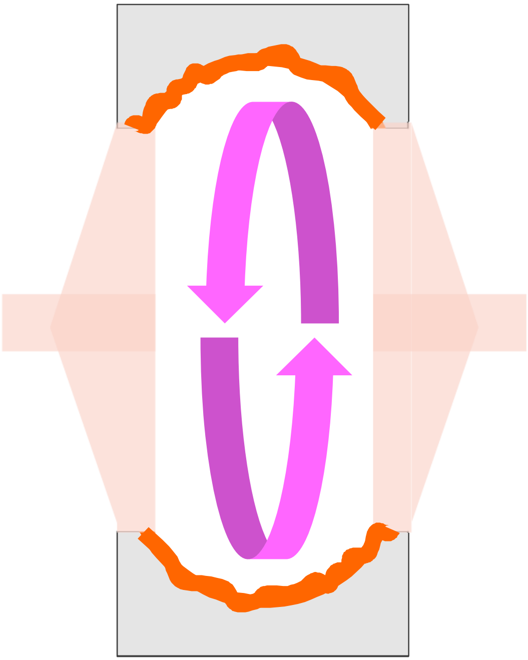

- Damping leads to length perturbation: fluctuation-dissipation theorem
  - off-resonant Brownian noise scales with mechanical loss in system
  - Brownian noise minimized via low-mechanical-loss materials

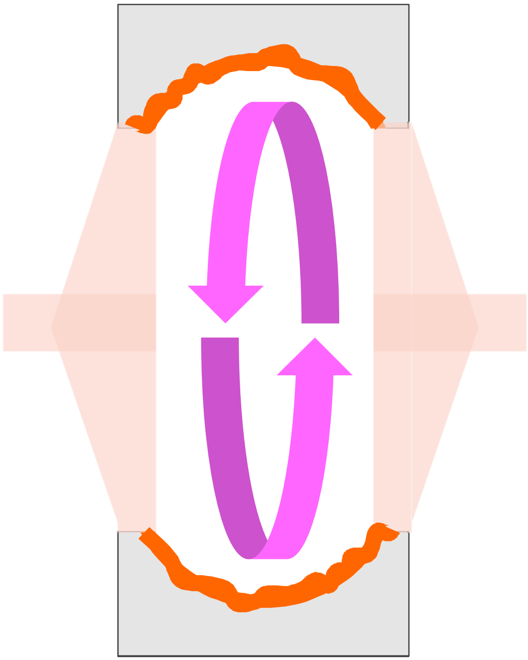

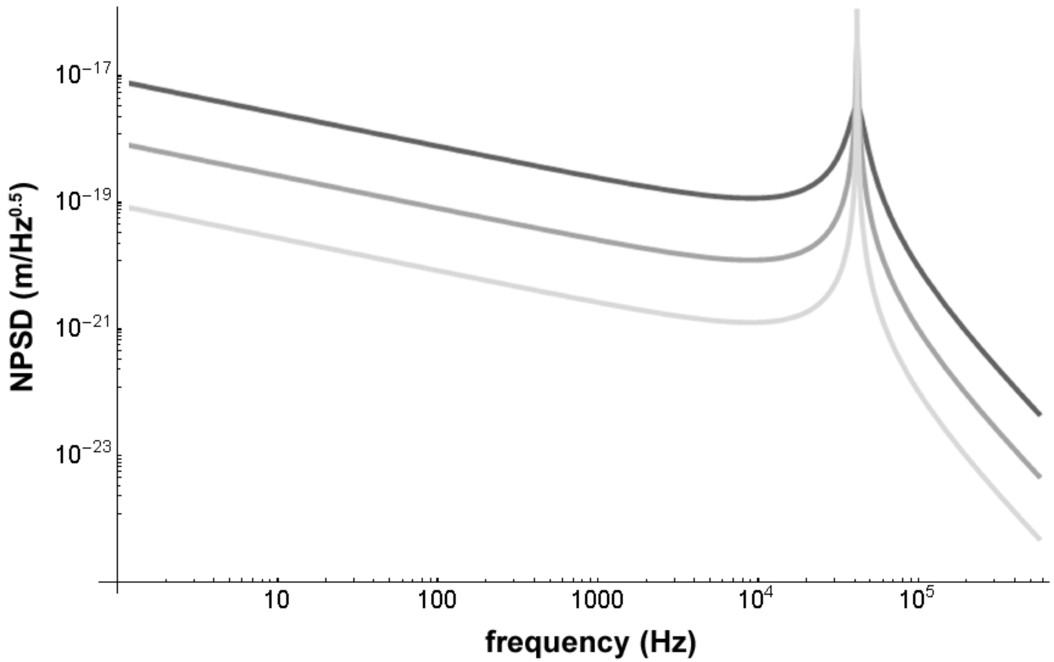

- Damping leads to length perturbation: fluctuation-dissipation theorem
  - off-resonant Brownian noise scales with mechanical loss in system
  - Brownian noise minimized via low-mechanical-loss materials

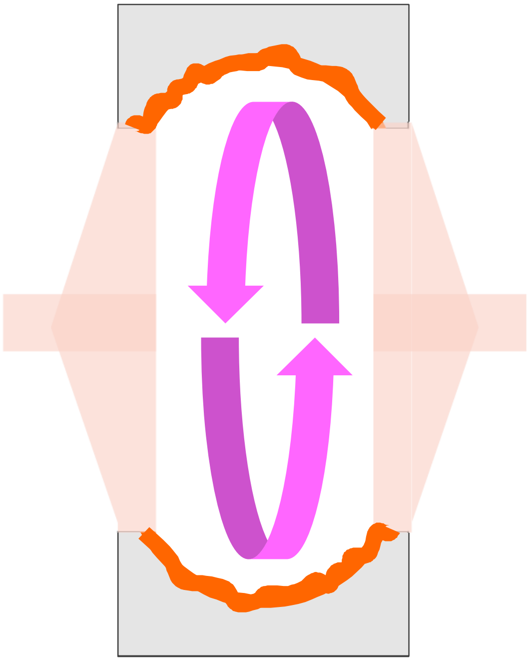

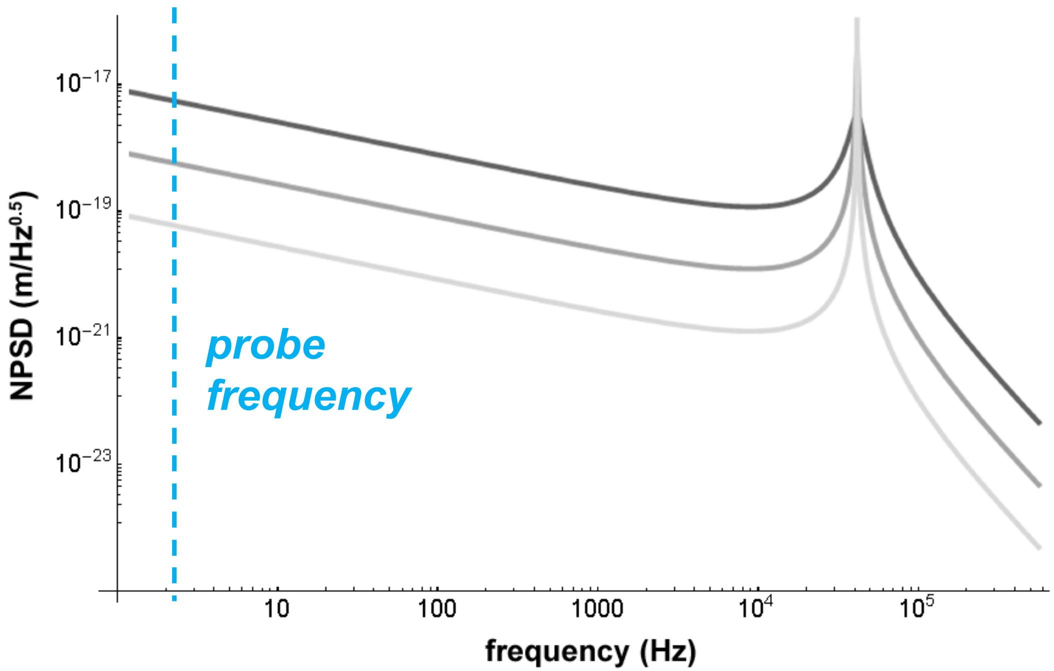

- Damping leads to length perturbation: fluctuation-dissipation theorem
  - off-resonant Brownian noise scales with mechanical loss in system
  - Brownian noise minimized via low-mechanical-loss materials

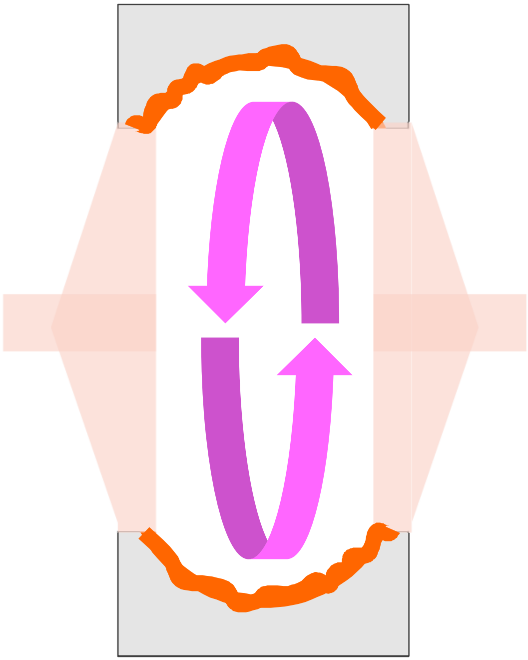

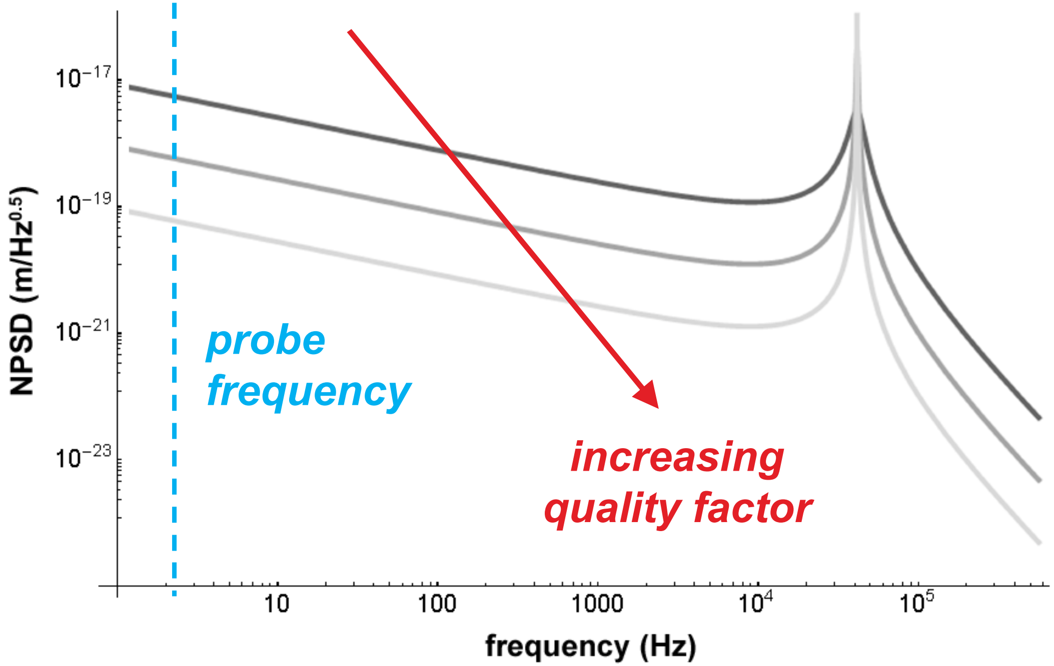

- Damping leads to length perturbation: fluctuation-dissipation theorem
  - off-resonant Brownian noise scales with mechanical loss in system
  - Brownian noise minimized via low-mechanical-loss materials

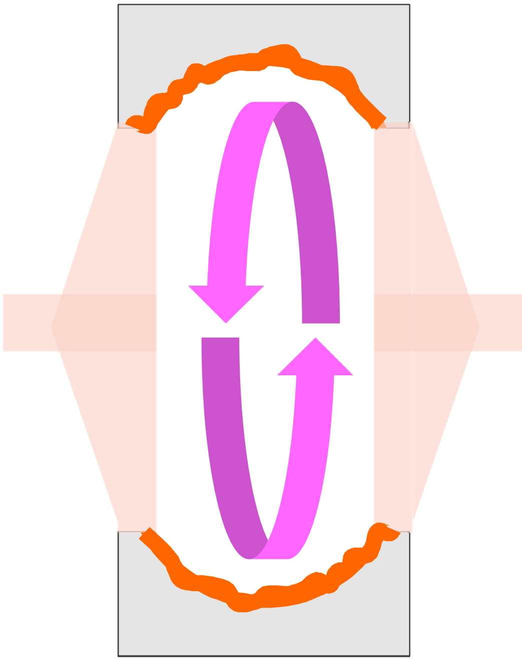

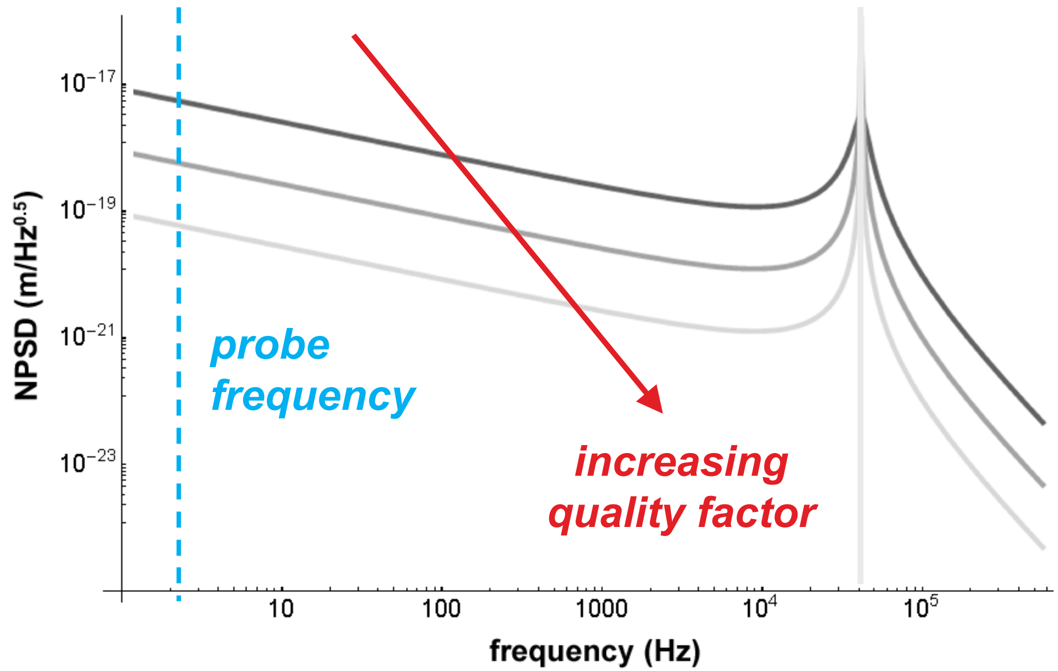

- Damping leads to length perturbation: fluctuation-dissipation theorem
  - off-resonant Brownian noise scales with mechanical loss in system
  - Brownian noise minimized via low-mechanical-loss materials

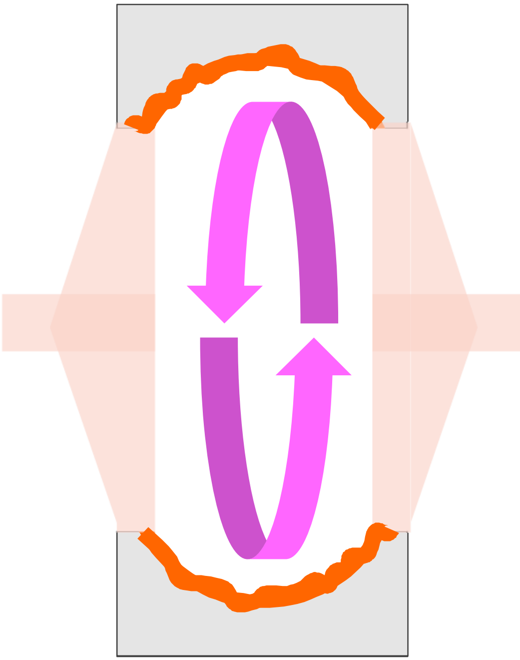

$$\delta_{x_t} = \left[\sum_{n=1}^{\infty} \frac{4 k_B T \phi \, \omega_n^2}{m_{eff,n} \, \omega \left[\left(\omega_n^2 - \omega^2 \right)^2 + \left(\phi \, \omega_n^2 \right)^2 \right]} \right]^{\frac{1}{2}}$$

P. R. Saulson, Phys. Rev. D 42, 2437 (1990)

- Damping leads to length perturbation: fluctuation-dissipation theorem
  - off-resonant Brownian noise scales with mechanical loss in system
  - Brownian noise minimized via low-mechanical-loss materials

Coating Thermal Noise Text Book

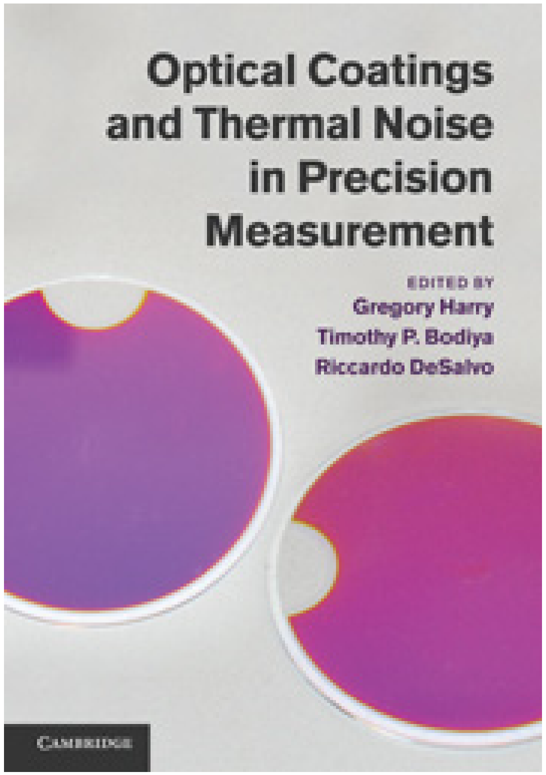

CAMBRIDGE UNIVERSITY PRESS

<u>Editors</u>:

Gregory Harry
American University, Washington DC

Timothy P. Bodiya
Massachusetts Institute of Technology

Riccardo DeSalvo
Università degli Studi del Sannio, Italy

Covers both the theoretical foundations and also implications of thermal noise in a variety of applications from GWDs, ultra-stable laser systems, cavity opto-mechanics, and cavity QED experiments

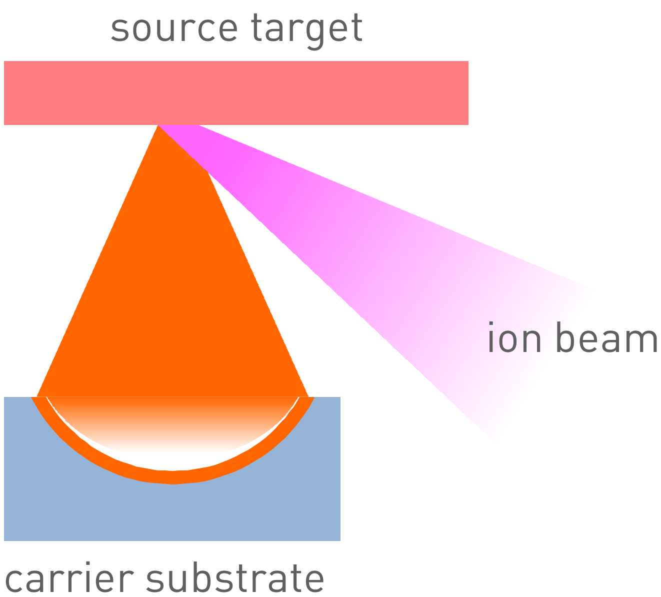

State-of-the-art multilayer mirrors:
ion-beam sputtered Ta_2O_5/SiO_2

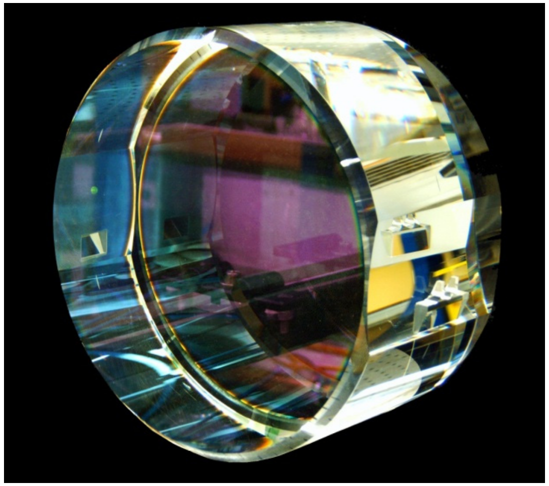

- Amorphous thin films deposited via ion beam sputtering (IBS)
  - pioneered by Litton Industries in the mid-1970s for RLGs
- Phenomenal optical properties: high R, low absorption and scatter
- Flexible choice of substrates and scalable manufacturing

- First demonstrated in 1975
  - interference coatings by van der Ziel and Ilegems, Bell Labs
- Primary application: VCSELs
  - K. Iga's group (Tokyo) and Bell Labs (Jewell, et al.)
  - VCSELs consist of high-reflectivity mirrors surrounding a semiconductor microcavity
  - global VCSEL market estimated to be worth $3.6B by Q4 2020
- Lattice matching constraints limit substrate selection
  - monocrystalline multilayers require a crystalline template

Substrate-emitting VCSEL (cross-section)

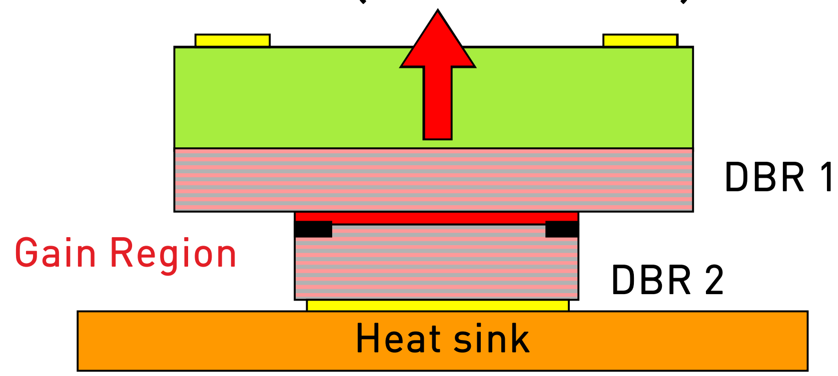

Large-aperture linear VCSEL array, Aerius Photonics, LLC (FLIR Electro-Optical Components)

Lattice Matched Epitaxial Multilayers

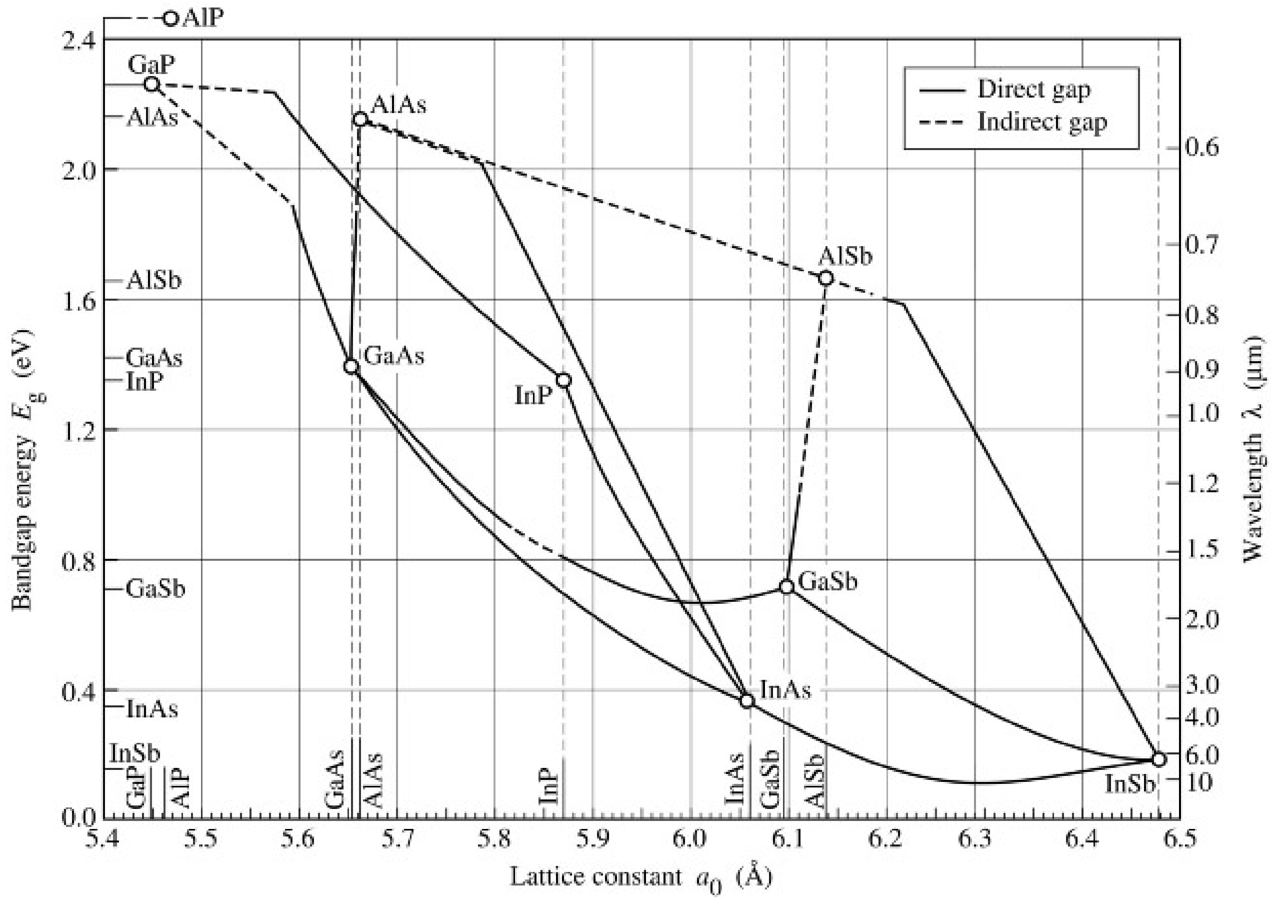

Material	Crystal structure	Lattice const. (A)	Modulus (GPa)	Density (kg/m^3)	CTE (x10^{-6} K^{-1})	Refractive index
GaAs	zinc blende	5.6455	85.3	5320	5.73	3.4804
AlAs	zinc blende	5.6533	83.5	3760	5.20	2.9383

Lattice Matched Epitaxial Multilayers

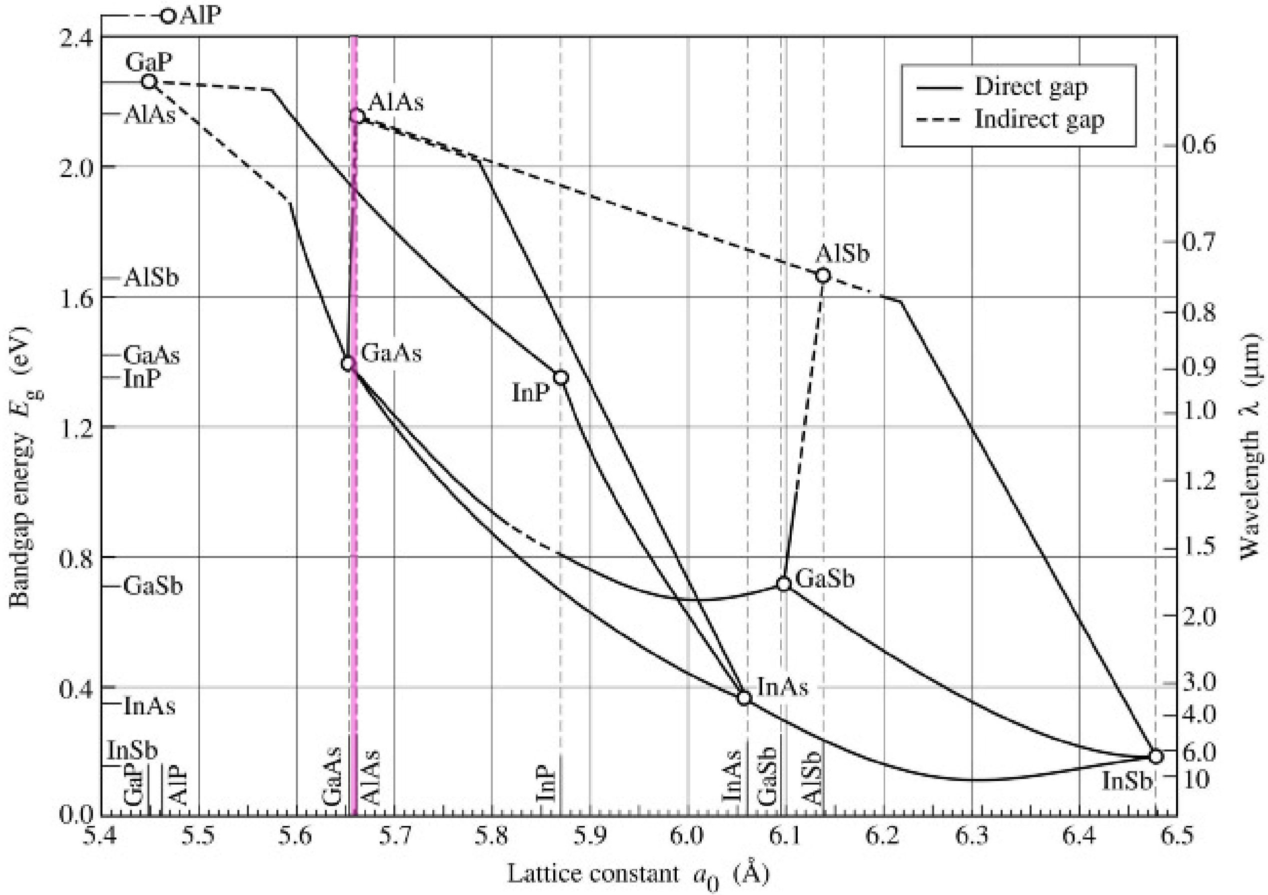

Material	Crystal structure	Lattice const. (A)	Modulus (GPa)	Density (kg/m^3)	CTE (x10^{-6} K^{-1})	Refractive index
GaAs	zinc blende	5.6455	85.3	5320	5.73	3.4804
AlAs	zinc blende	5.6533	83.5	3760	5.20	2.9383

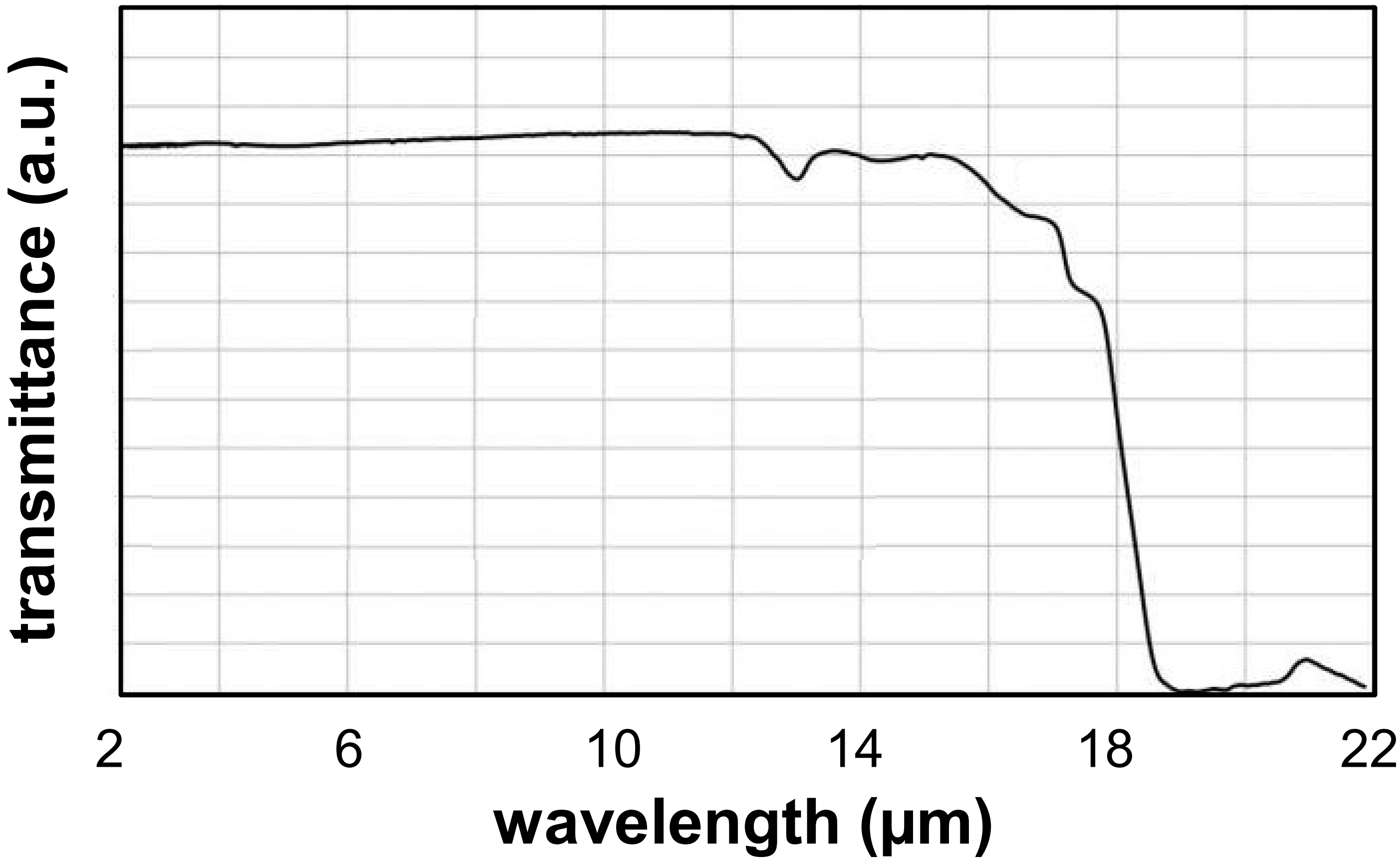

- GaAs is a commonly used material for mid and long-wave optics
  - what losses can be expected from GaAs/AlGaAs multilayers?

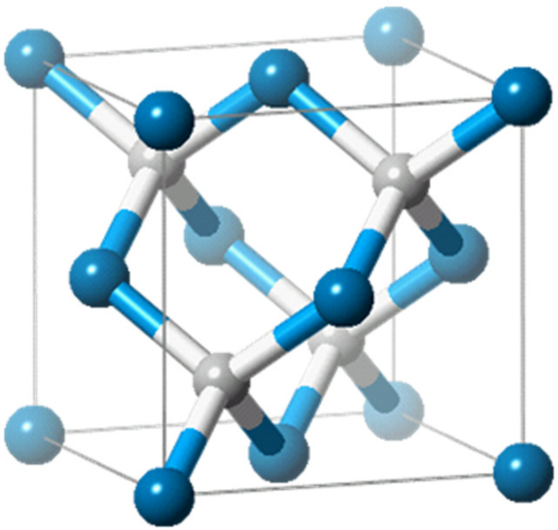

Zinc blende unit cell with cubic symmetry yielding three elastic constants: c11, c12, & c44

$$c_{IJ} = \begin{bmatrix} c_{11} & c_{12} & c_{12} & & & \\ c_{12} & c_{11} & c_{12} & & & \\ c_{12} & c_{12} & c_{11} & & & \\ & & & c_{44} & & \\ & & & & c_{44} & \\ & & & & & c_{14} \end{bmatrix}$$

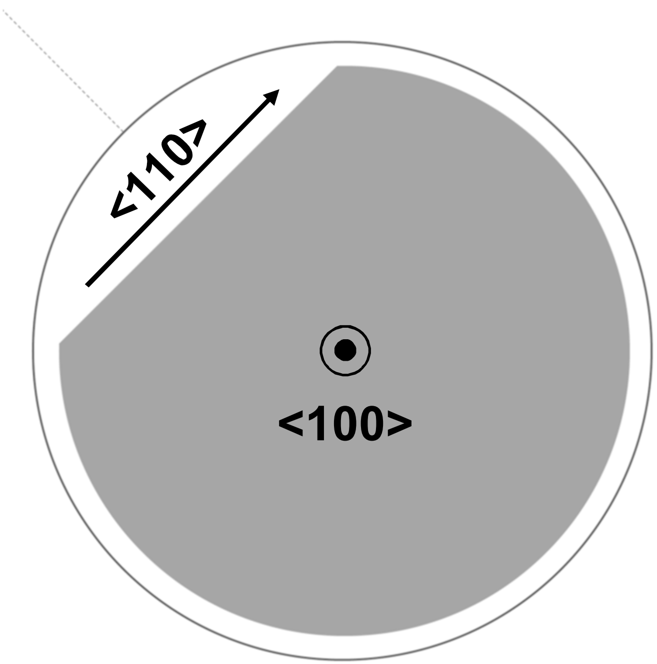

Current orientation is <100> (surface normal)

$$Y_{100} = c_{11} - 2\left(\frac{{c_{12}}^2}{c_{11} + c_{12}}\right)$$

$$Y_{110} = 4\left(\frac{c_{44}({c_{11}}^2 + c_{11}c_{12} - 2{c_{12}}^2)}{{c_{11}}^2 + c_{11}c_{12} + 2c_{11}c_{44} - 2c_{12}}\right)$$

$$Y_{111} = 3\left(\frac{c_{44}(c_{11} + 2c_{12})}{c_{11} + 2c_{12} + c_{44}}\right)$$

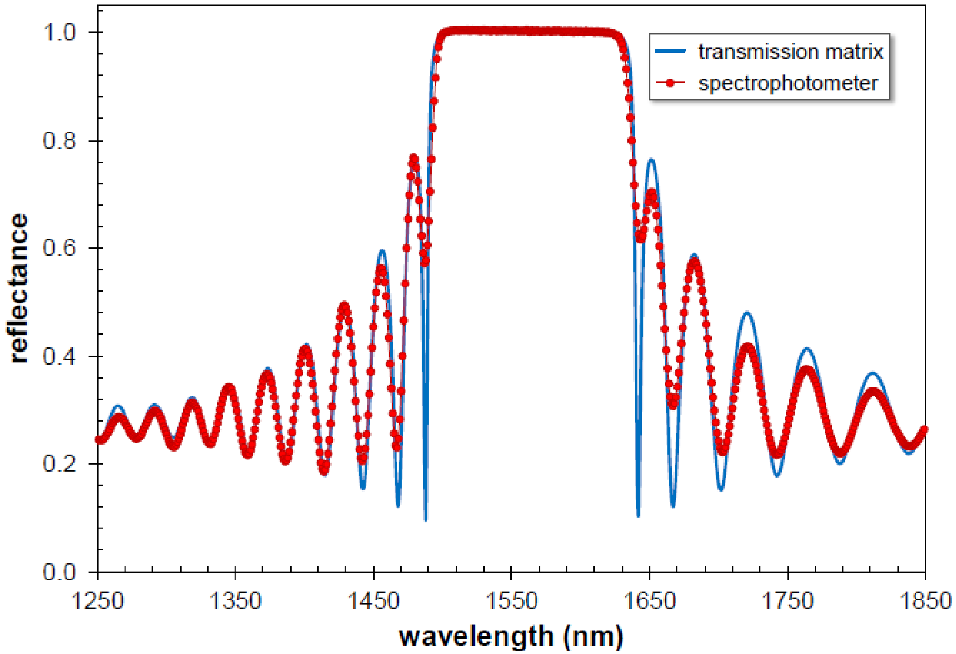

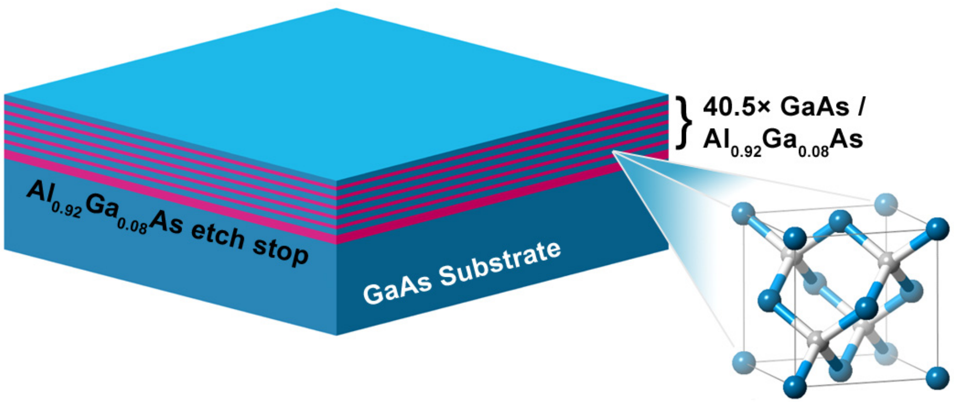

- AlGaAs multilayer with varying Al content for index contrast
  - high index layers consist of binary GaAs thin films
  - 8% Ga incorporated in low index AlGaAs layers to slow oxidation in ambient
- Epitaxy generates DBRs with low defect density, high purity, and excellent thickness control
  - limited by lattice matching…
- Leverage transfer & direct bonding to overcome this
  - commonly employed process, e.g. for manufacturing SOI (silicon-on-insulator) wafers up to 45 cm in diameter

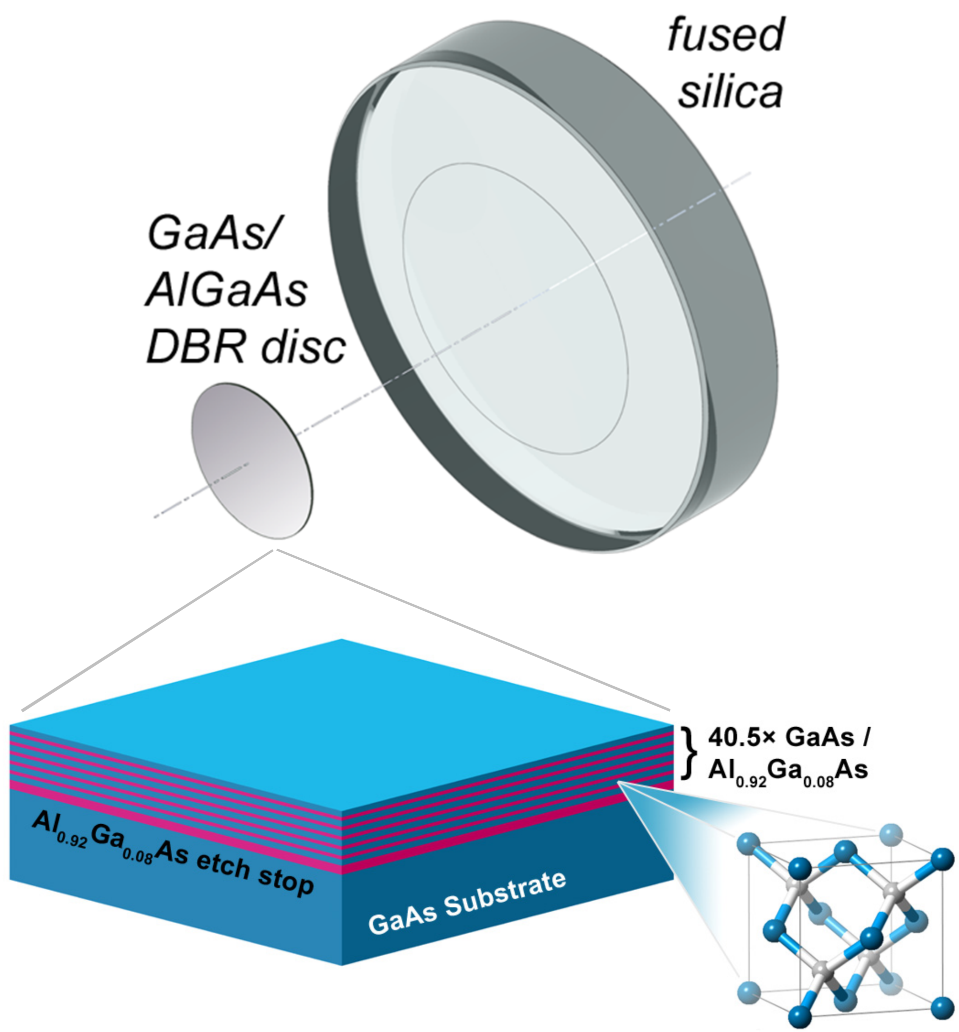

- AlGaAs multilayer with varying Al content for index contrast
    - high index layers consist of binary GaAs thin films
    - 8% Ga incorporated in low index AlGaAs layers to slow oxidation in ambient
- Epitaxy generates DBRs with low defect density, high purity, and excellent thickness control
    - limited by lattice matching...
- Leverage transfer & direct bonding to overcome this
    - commonly employed process, e.g. for manufacturing SOI (silicon-on-insulator) wafers up to 45 cm in diameter

First Demonstration of a Reference Cavity w/ Crystalline Coatings

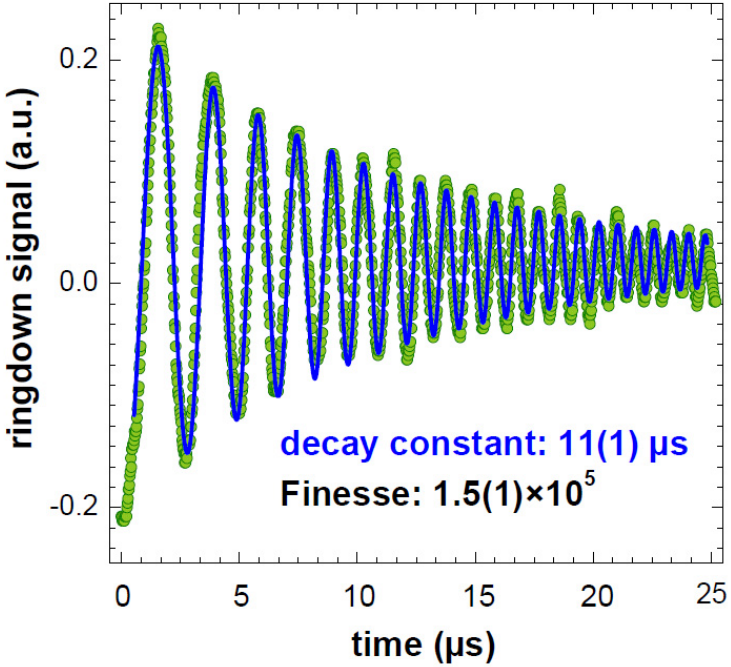

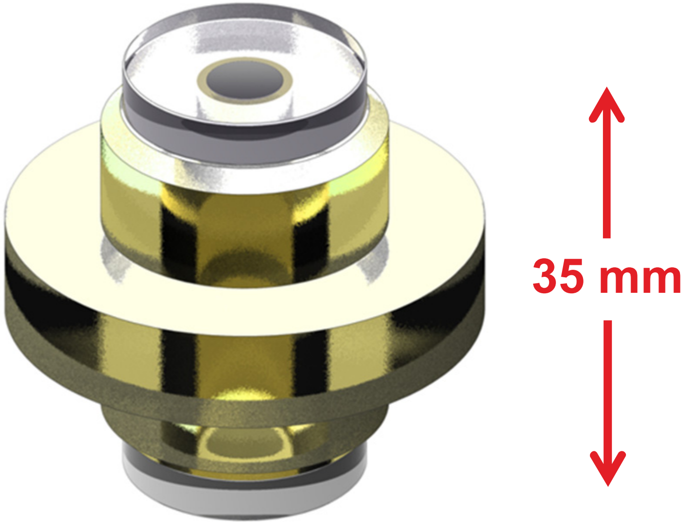

- Optical cavity ringdown yields a finesse of 150,000 @ 1064 nm
  - transmission of ~5 ppm, scatter + absorption loss of 15 ppm
- Extracted quality factor matches measurements on µ-resonators
  - coating loss angle below 4×10^{-5} (potential for $<5 \times 10^{-6}$ at cryo)

G. D. Cole, W. Zhang, M. J. Martin, J. Ye, and M. Aspelmeyer, Nature Photonics (2013)

First Demonstration of a Reference Cavity w/ Crystalline Coatings

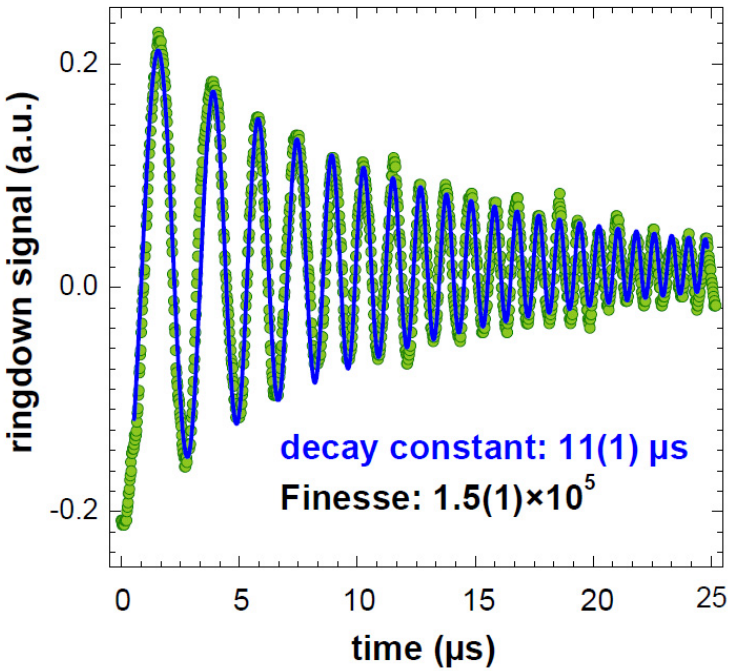

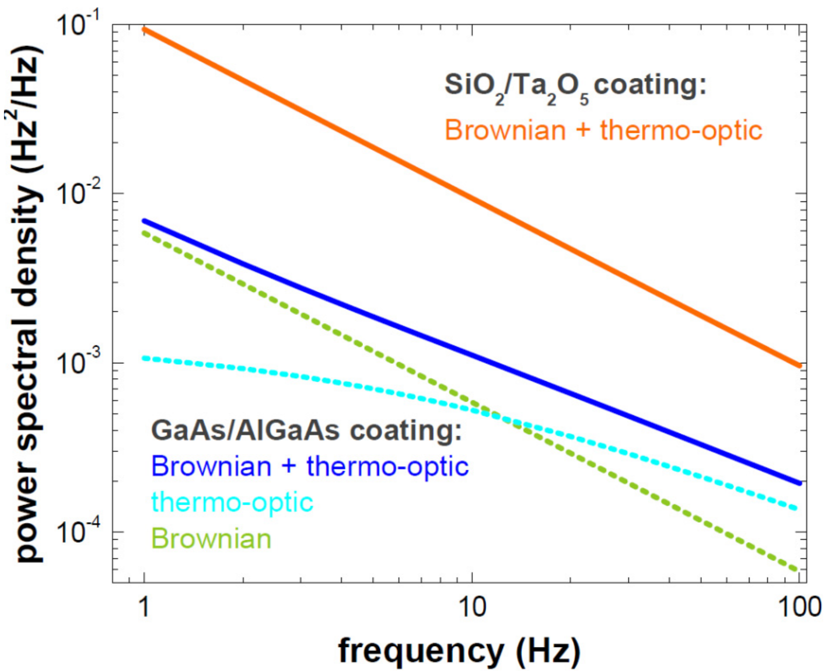

- Optical cavity ringdown yields a finesse of 150,000 @ 1064 nm
  - transmission of ~5 ppm, scatter + absorption loss of 15 ppm
- Extracted quality factor matches measurements on μ-resonators
  - coating loss angle below 4×10^{-5} (potential for $<5 \times 10^{-6}$ at cryo)

G. D. Cole, W. Zhang, M. J. Martin, J. Ye, and M. Aspelmeyer, Nature Photonics (2013)

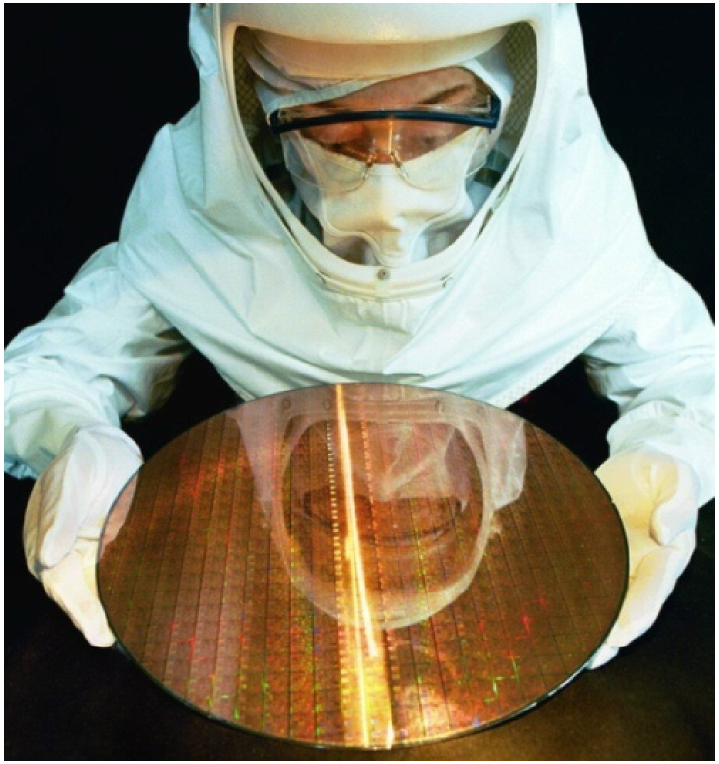

Merging Semiconductor Manufacturing with Bulk Optics

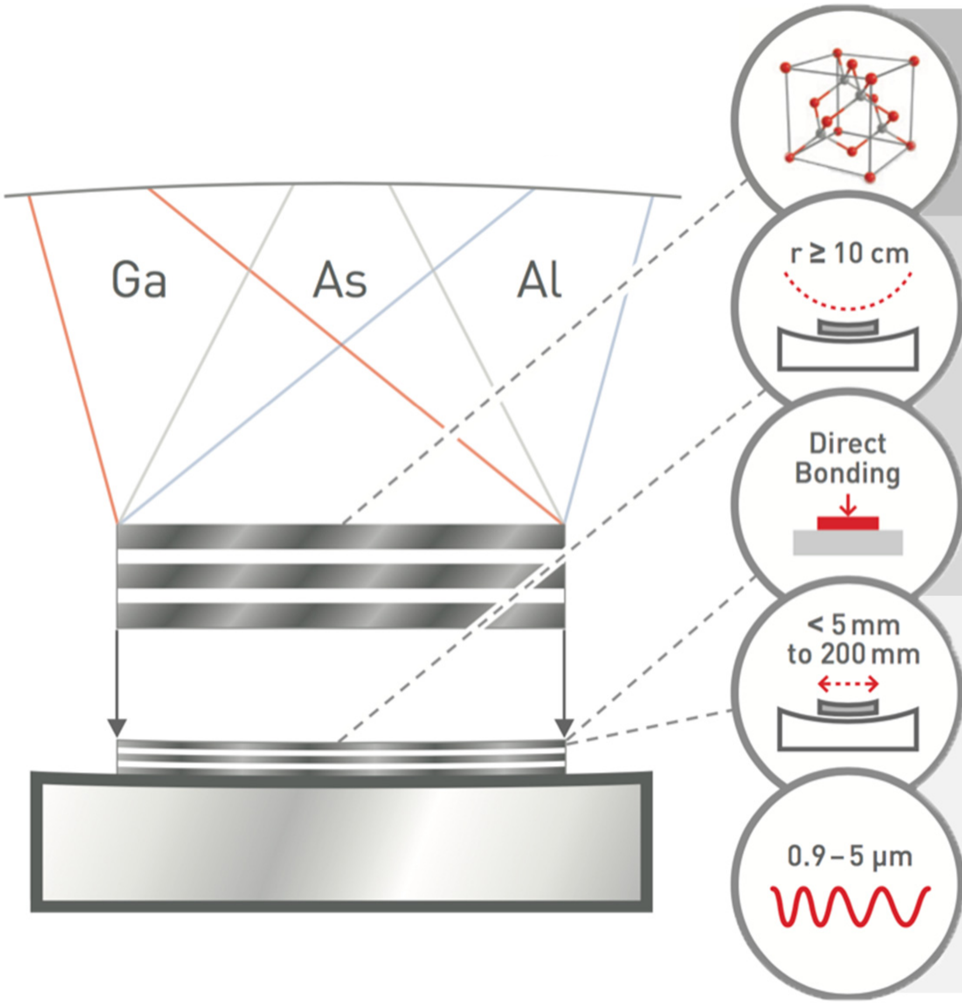

Monocrystalline GaAs/AlGaAs heterostructures grown on GaAs wafers by molecular beam epitaxy

Using semiconductor manufacturing techniques, the multilayer is extracted from the original GaAs wafer

Direct bonding is used to attach the single-crystal interference coating to the final optical substrate

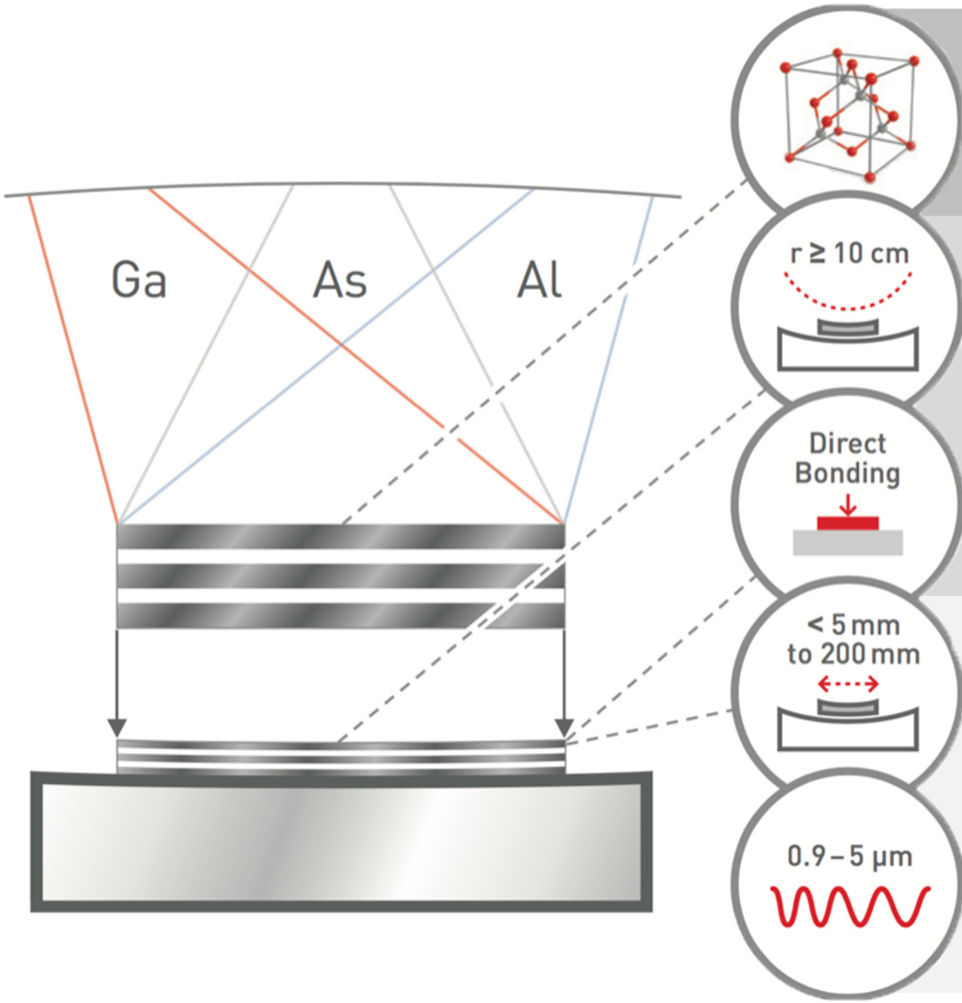

Monocrystalline GaAs/AlGaAs heterostructures grown on GaAs wafers by molecular beam epitaxy

Using semiconductor manufacturing techniques, the multilayer is extracted from the original GaAs wafer

Direct bonding is used to attach the single-crystal interference coating to the final optical substrate

Epitaxial multilayers on arbitrary substrates

3 key advantages:

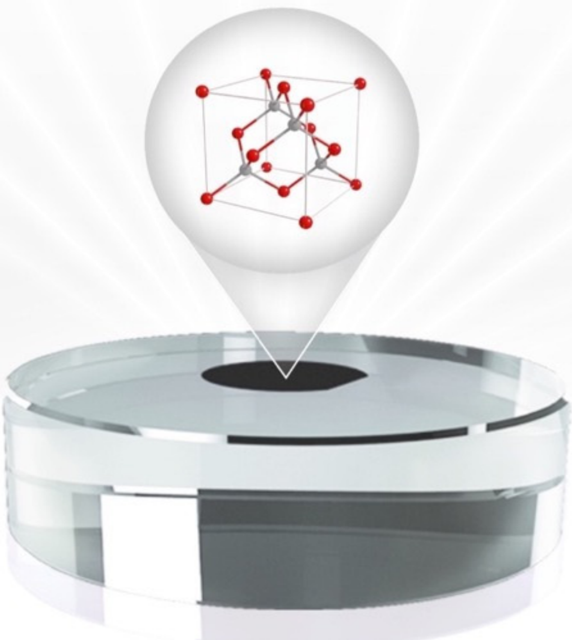

10x LOWER Brownian noise — ULTRAPRECISE measurements of space and time

10x LOWER mid-infrared absorption — HIGH RESOLUTION trace gas sensing

30x LOWER thermal resistivity — THERMAL MANAGEMENT in industrial lasers

- Introduction to substrate-transferred crystalline coatings
- **Microfabrication-based coating process overview**
- Advantages of bonded single-crystal interference coatings
  - low elastic losses and minimal Brownian noise
  - mid-infrared optical transparency
  - high thermal conductivity

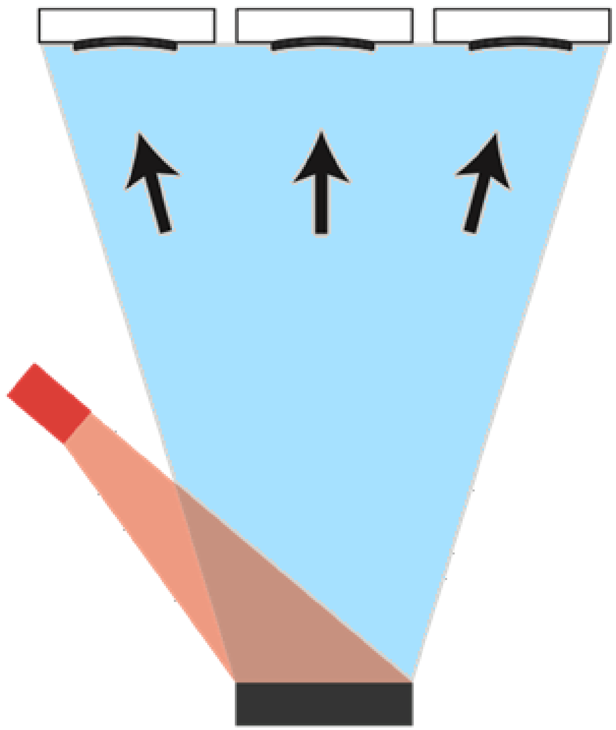

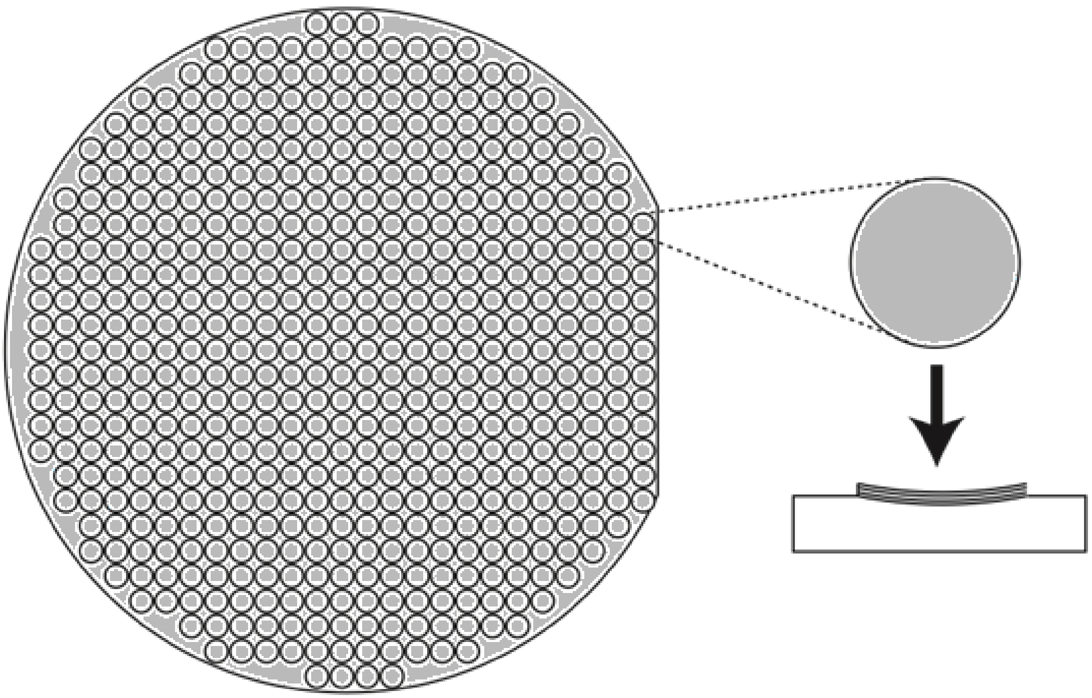

Physical vapor deposition can be realized on multiple substrates simultaneously

Wafer-scale batch fabrication enables the generation of many GaAs/AlGaAs mirror disks, though bonding (currently) remains a serial process

GaAs wafers (seed crystal)

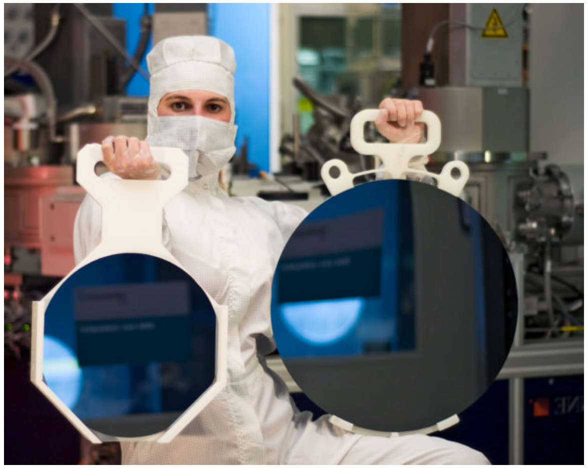

Crystal growth via MBE

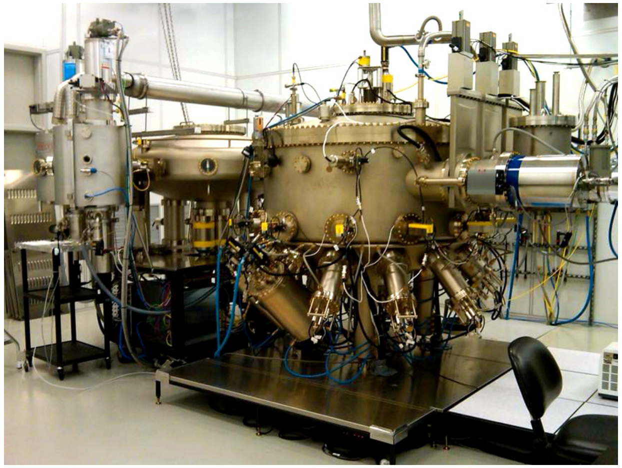

Microfab & bonding

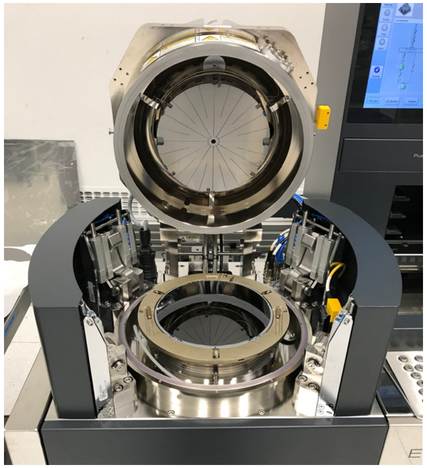

- Crystalline coatings entail a unique manufacturing process
  - we purchase base GaAs wafers from an external supplier
  - epitaxial growth of a custom designed multilayer w/ MBE
  - using a proprietary process we remove and directly bond the single-crystal multilayer to a super-polished substrate

Epitaxial Growth Options

Molecular beam epitaxy

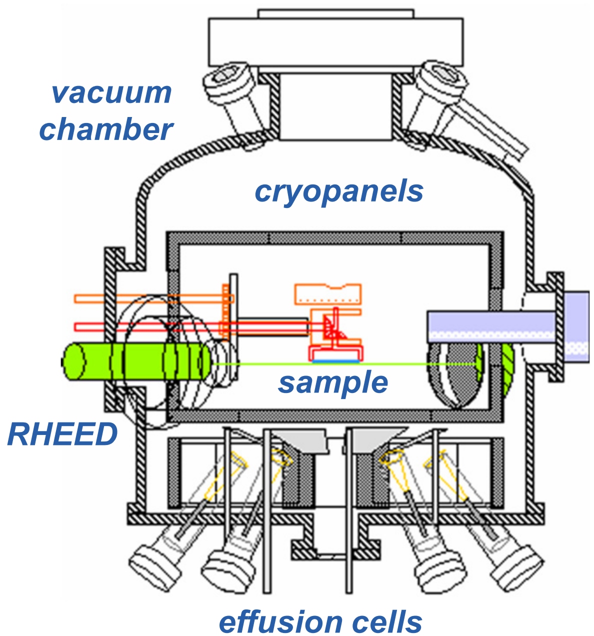

Metal organic chemical vapor deposition

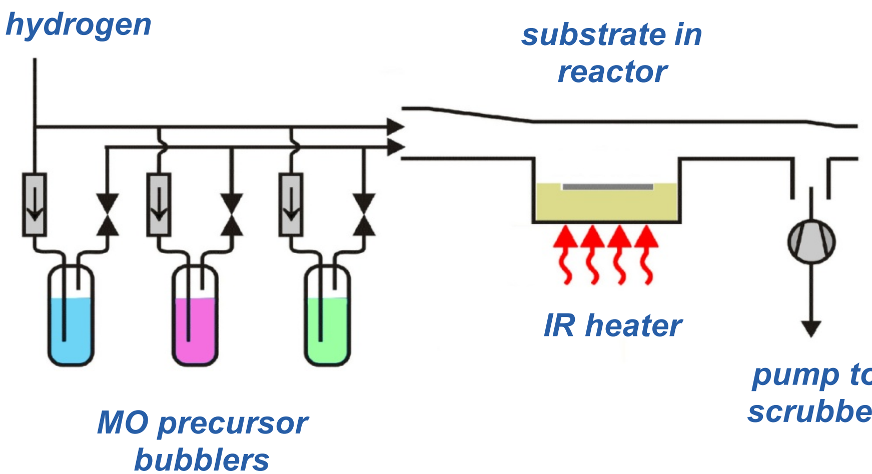

- MBE enables low background doping, minimizing absorption
- Oval defects in GaAs (spitting Ga source) are a persistent problem

- C incorporation in AlGaAs is a major barrier to achieving low absorption
- An optimized MOCVD process can generate defect free films

Molecular beam epitaxy

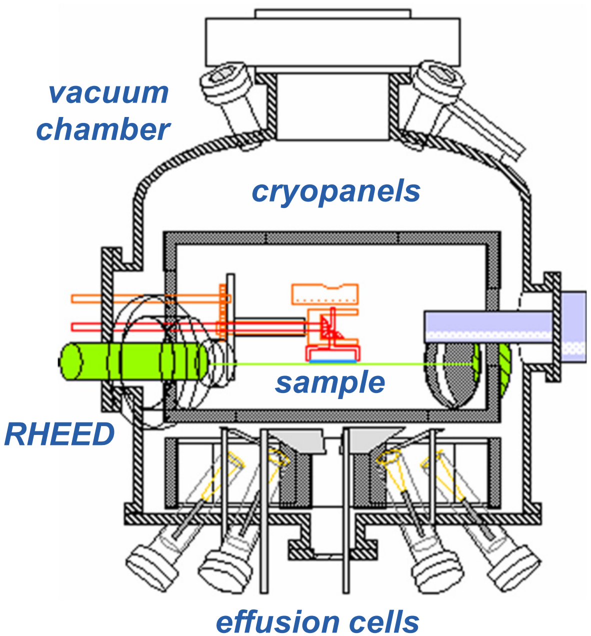

- MBE enables low background doping, minimizing absorption
- Oval defects in GaAs (spitting Ga source) are a persistent problem

Metal organic chemical vapor deposition

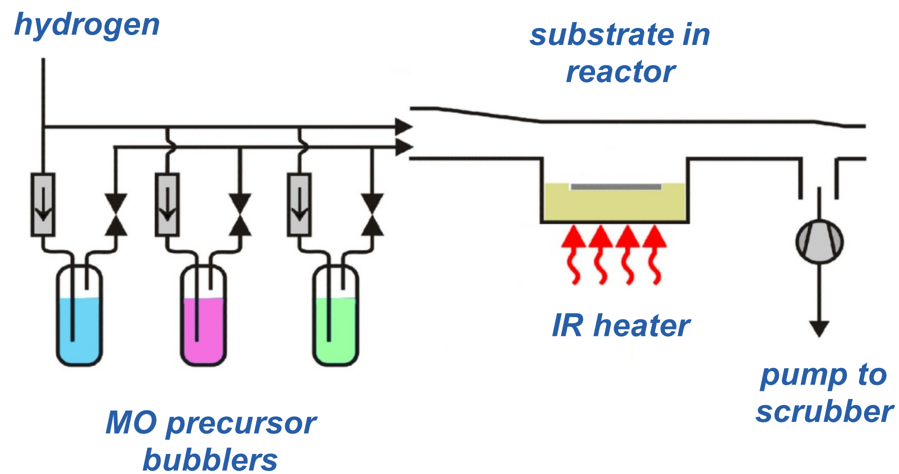

- C incorporation in AlGaAs is a major barrier to achieving low absorption
- An optimized MOCVD process can generate defect free films

First Large-Area Coating Runs 2016/2017

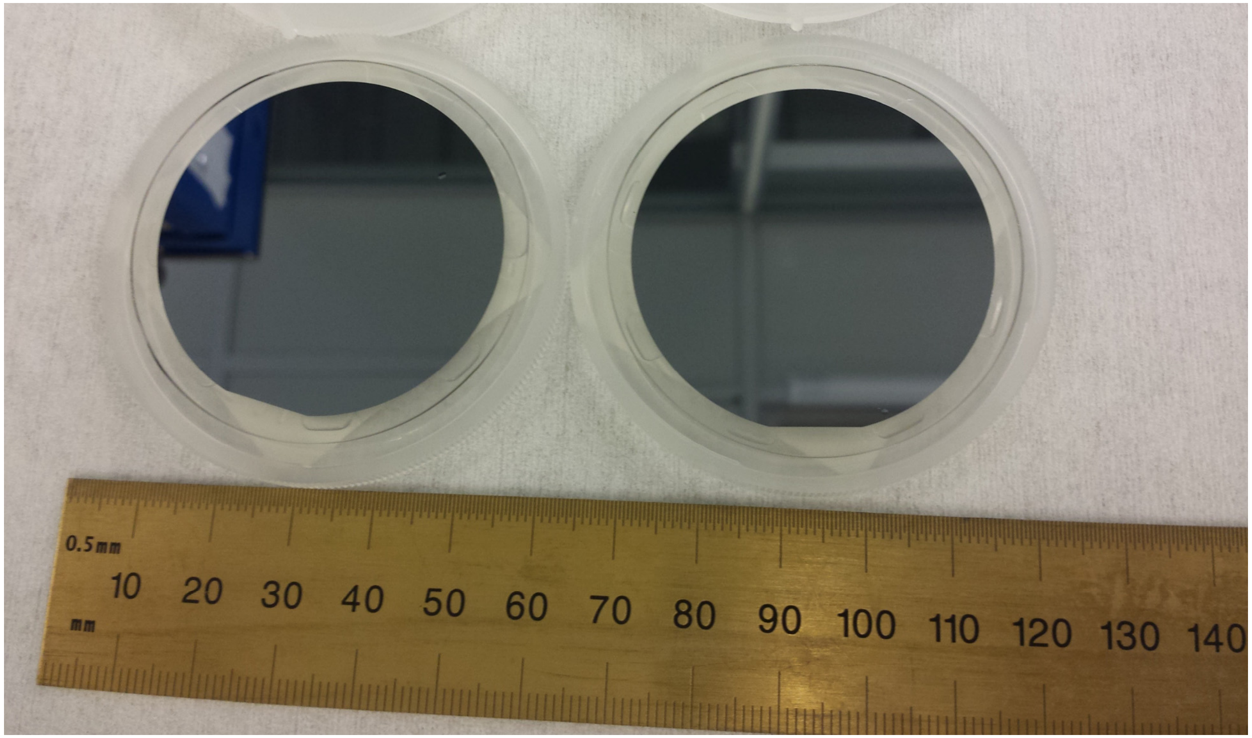

- High reflectivity 1064 nm crystalline coatings on fused silica wafers
  - 35.5 period mirror, target transmission of 10 ppm at normal incidence
- Samples used for process evaluation and in-depth characterization
  - properties of interest include optical scatter and thickness uniformity

Substrate-Transfer Process: Step 1, Litho and Etch

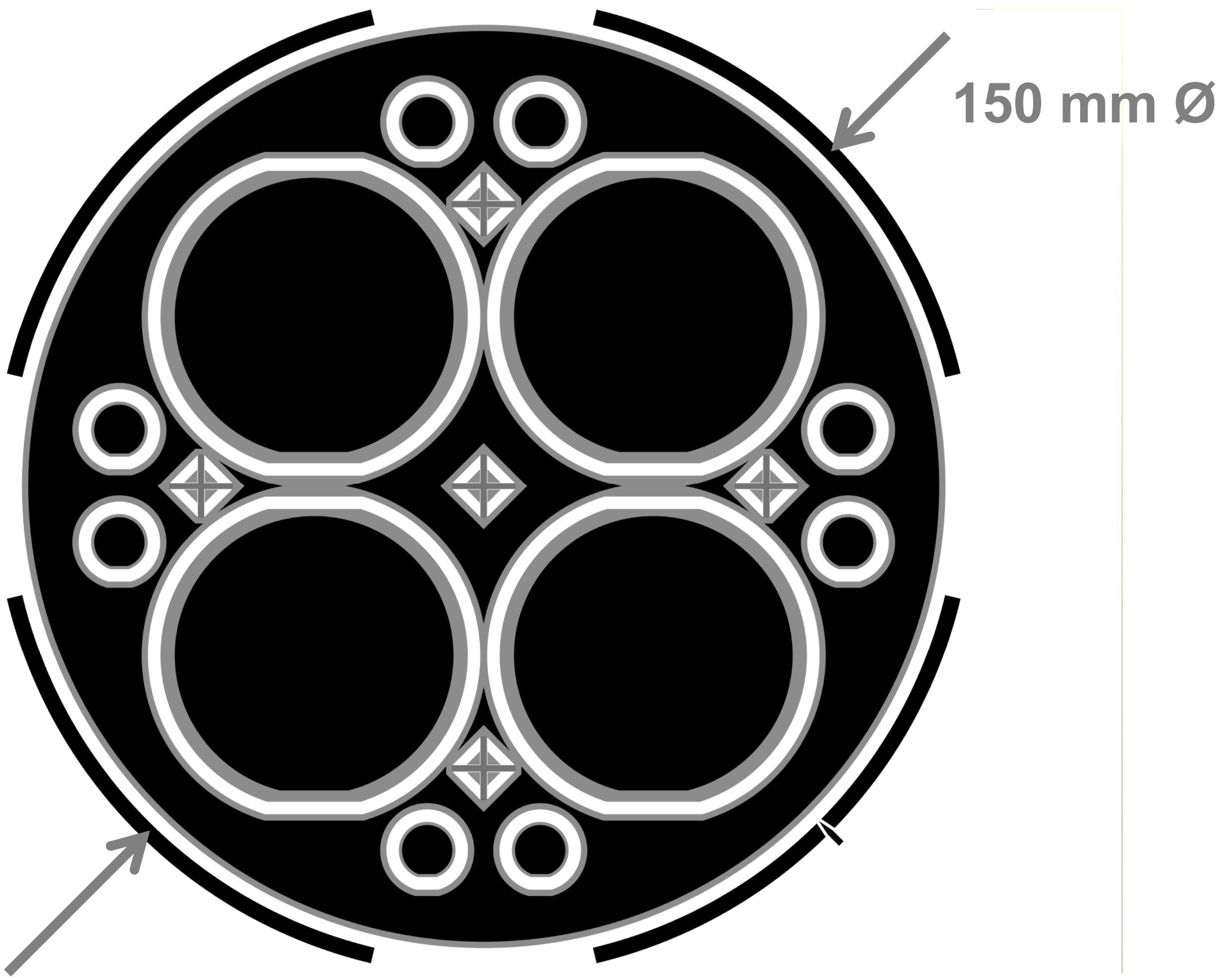

Substrate-Transfer Process: Step 1, Litho and Etch

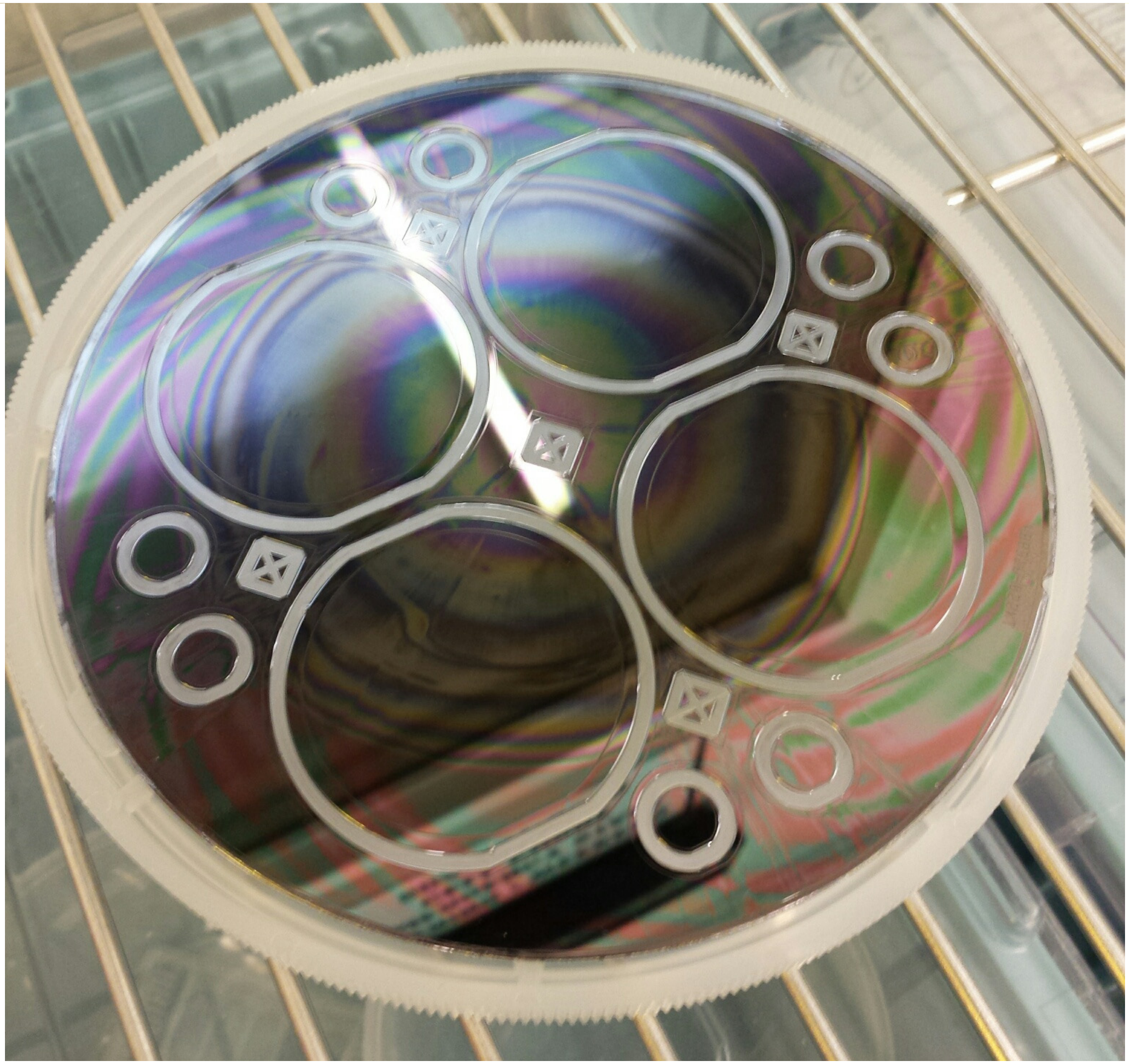

Step 2: Die Singulation via Lapping

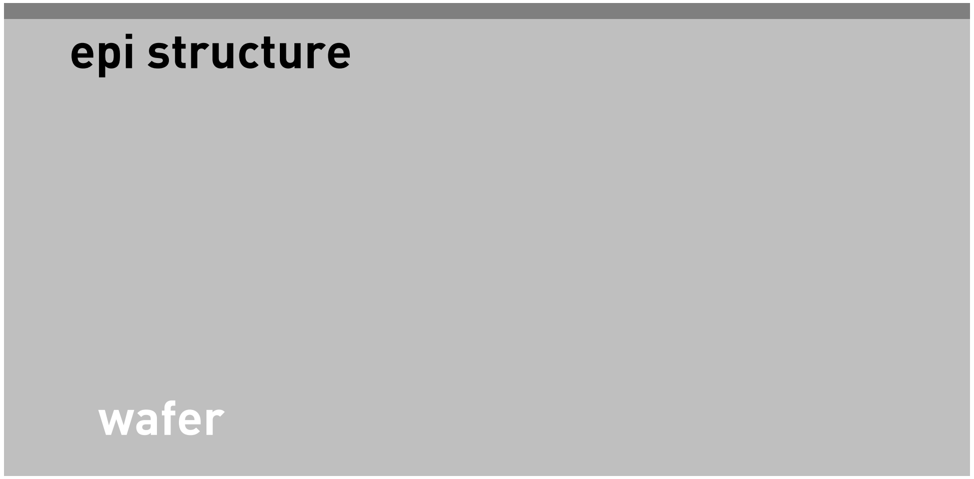

- Contact lithography is used to define the coating geometry
  - a non-selective wet etch (H_3PO_4:H_2O_2:H_2O) transfers this pattern into the DBR and partially into the GaAs wafer
- A second mask is used to define a slightly larger mesa
  - the same chemistry is used to deep etch (150-250 μm) into the substrate, which is typically 675 μm thick
- Lapping is used to thin the underlying wafer to ~100 μm
  - singulated die are generated with excellent control of the lateral geometry

Step 2: Die Singulation via Lapping

- Contact lithography is used to define the coating geometry
    - a non-selective wet etch (H_3PO_4:H_2O_2:H_2O) transfers this pattern into the DBR and partially into the GaAs wafer
- A second mask is used to define a slightly larger mesa
    - the same chemistry is used to deep etch (150-250 μm) into the substrate, which is typically 675 μm thick
- Lapping is used to thin the underlying wafer to ~100 μm
    - singulated die are generated with excellent control of the lateral geometry

Step 2: Die Singulation via Lapping

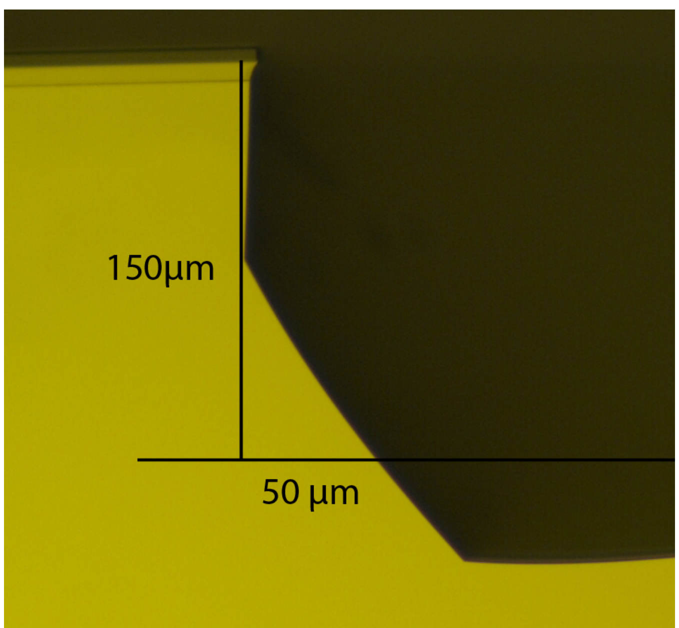

- Contact lithography is used to define the coating geometry
  - a non-selective wet etch (H_3PO_4:H_2O_2:H_2O) transfers this pattern into the DBR and partially into the GaAs wafer
- A second mask is used to define a slightly larger mesa
  - the same chemistry is used to deep etch (150-250 µm) into the substrate, which is typically 675 µm thick
- Lapping is used to thin the underlying wafer to ~100 µm
  - singulated die are generated with excellent control of the lateral geometry

Step 2: Die Singulation via Lapping

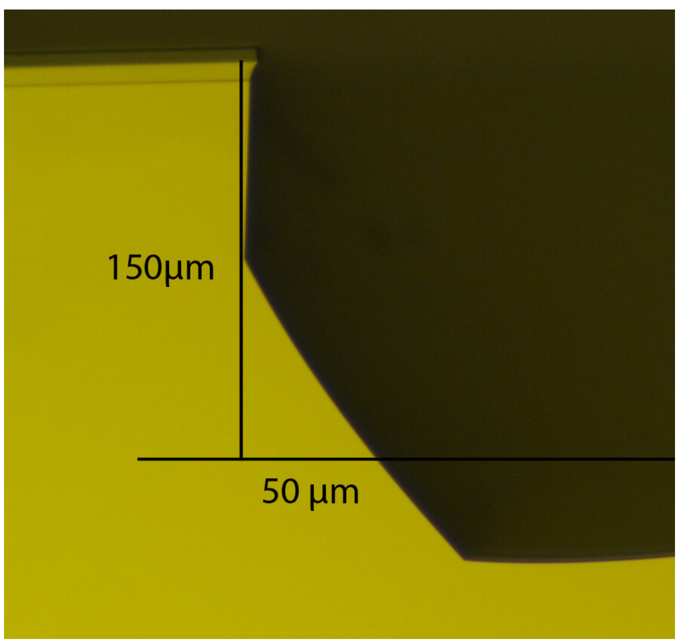

- Contact lithography is used to define the coating geometry
  - a non-selective wet etch (H_3PO_4:H_2O_2:H_2O) transfers this pattern into the DBR and partially into the GaAs wafer
- A second mask is used to define a slightly larger mesa
  - the same chemistry is used to deep etch (150-250 µm) into the substrate, which is typically 675 µm thick
- Lapping is used to thin the underlying wafer to ~100 µm
  - singulated die are generated with excellent control of the lateral geometry

Step 3: Direct Bonding of Cleaned and Activated Components

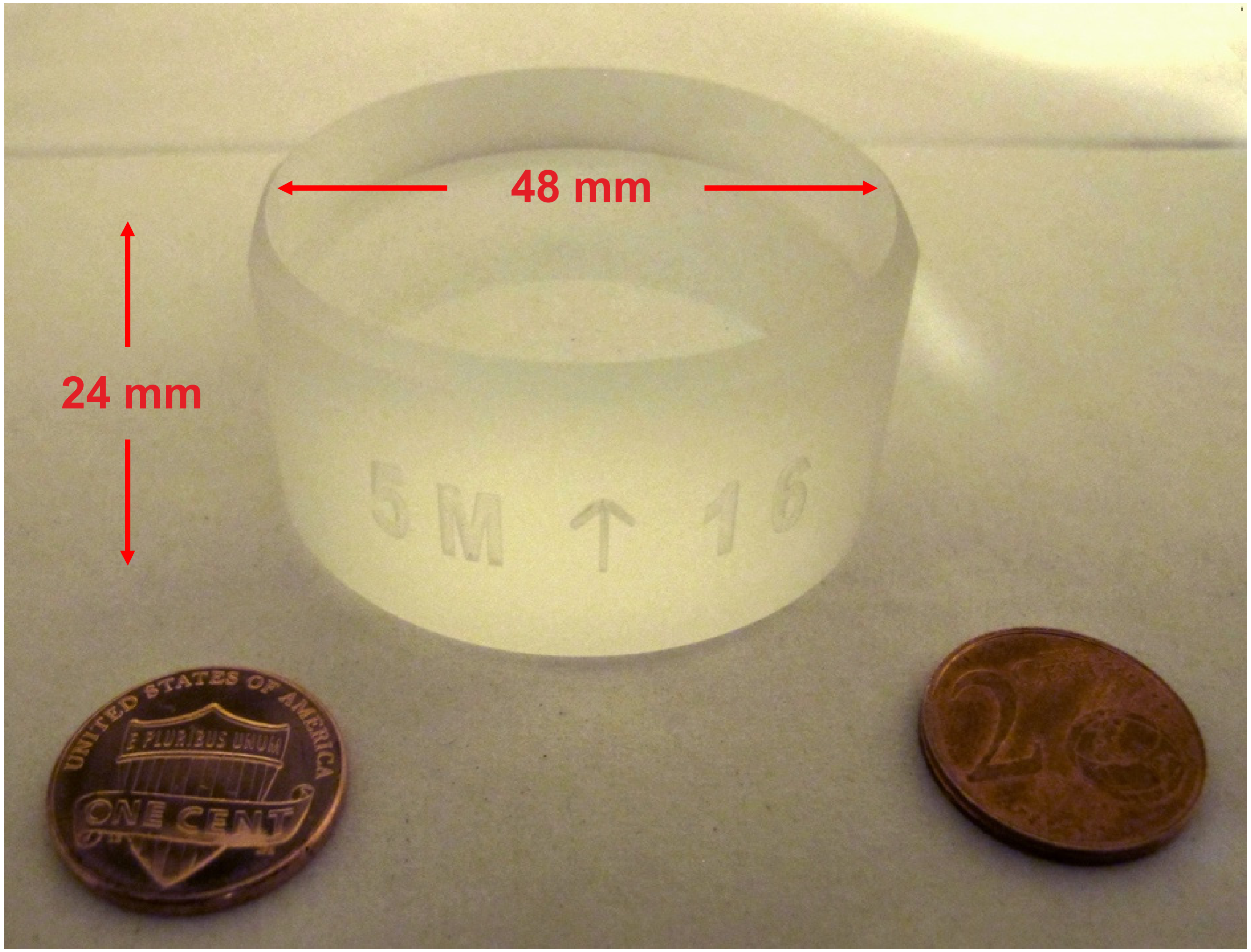

Step 3: Direct Bonding of Cleaned and Activated Components

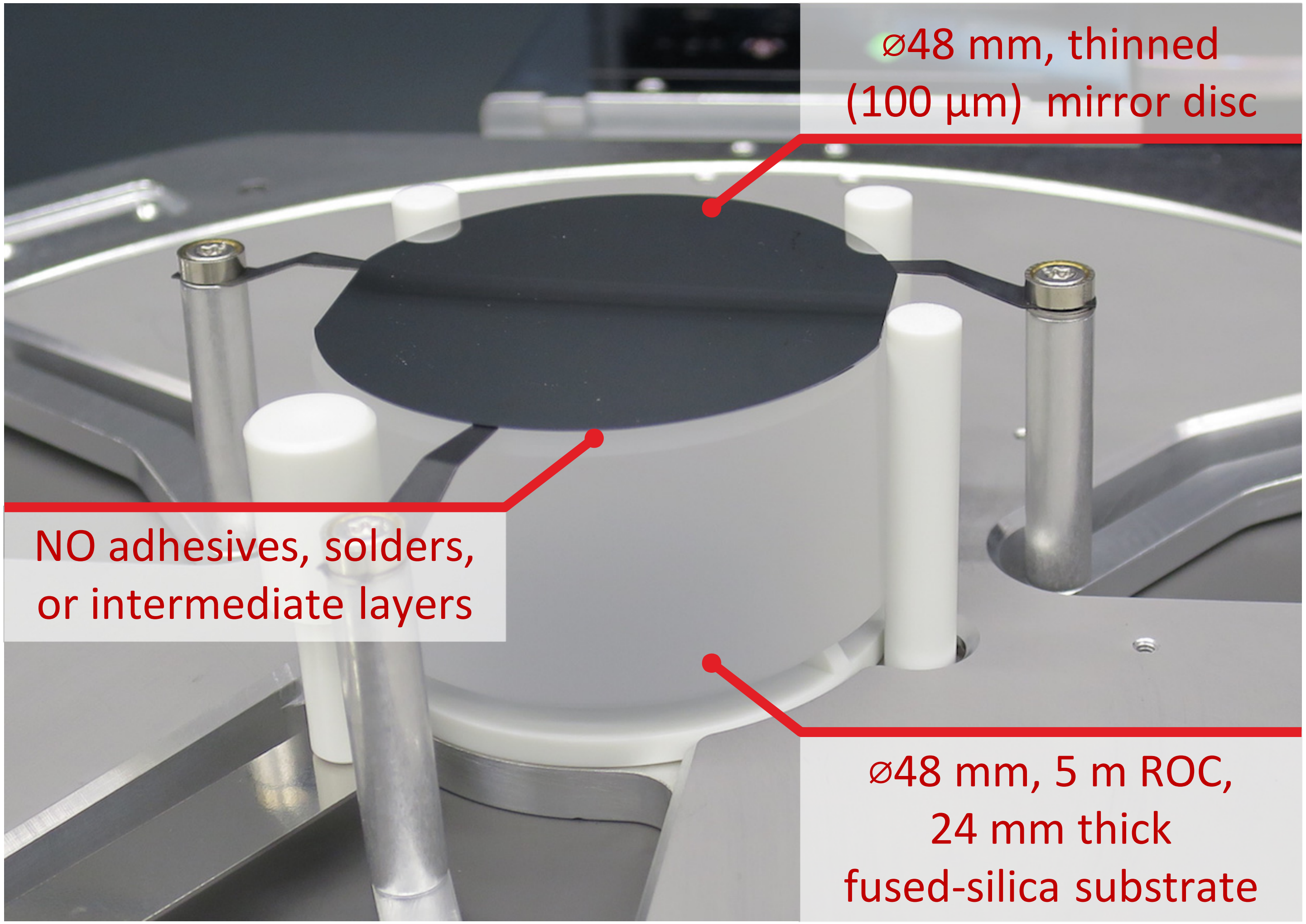

Steps 4 and 5: Substrate Removal and Final Cleaning

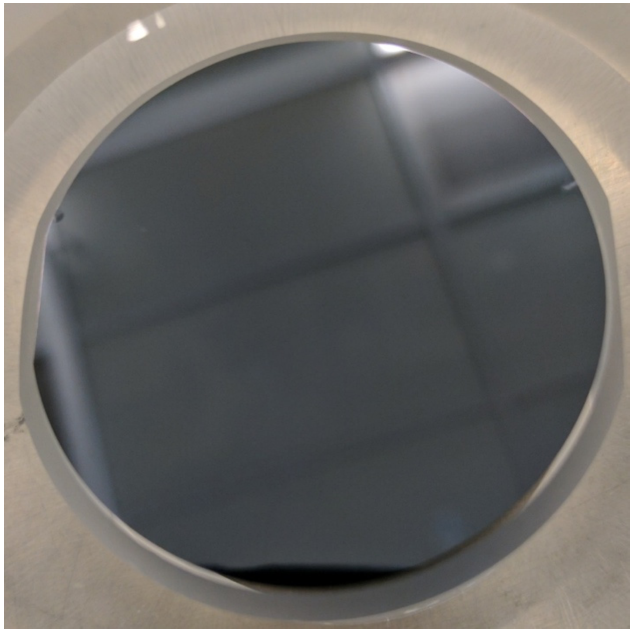

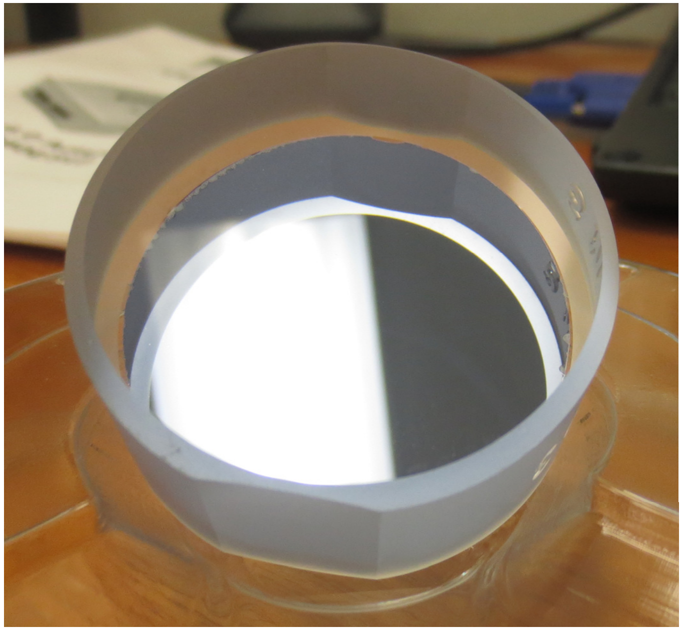

- High optical performance realized with acceptable yield
  - typical crystalline coatings are 0.5-1 inch in diameter
  - maximum delivered coating diameter to date is 3" / 76.2 mm
  - we can successfully transfer epilayers onto surfaces w/ a 10-cm ROC

Optical and Noise Performance of Large-Area Coatings

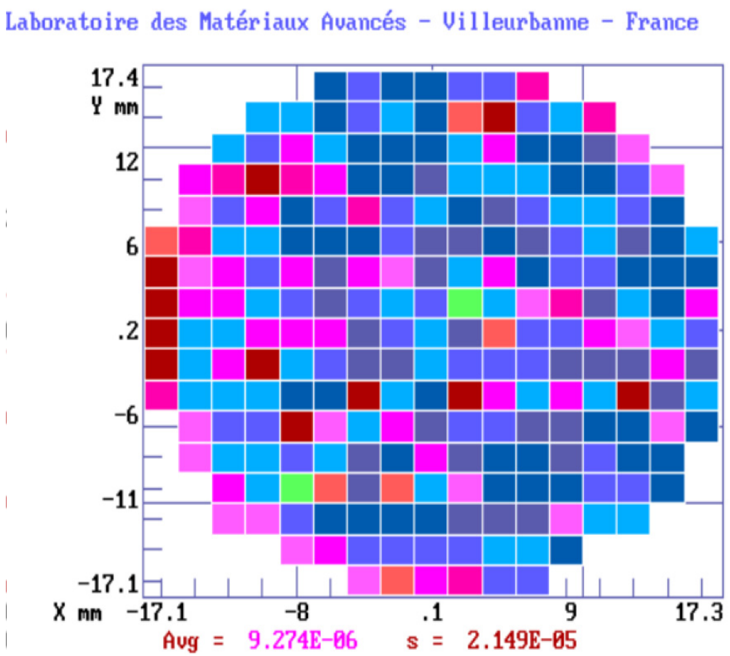

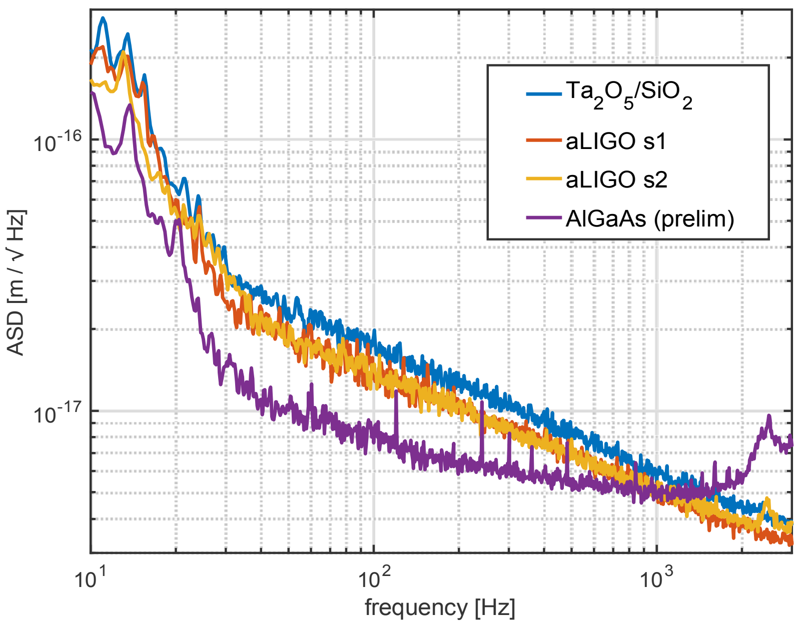

Measurement	Coating on silica substrate	Coating on sapphire substrate
Transmission @1064 nm	6 ppm	6 ppm
Absorption @1064 nm	≤ 0.8 ppm	below the noise floor
Scattering @1064 nm	9.5 ppm	6 ppm
Coating Roughness	7.7 Å RMS	1.1 Å RMS
Substrate Roughness	9.1 Å RMS	1.1 Å RMS

Marchio et al., Optics Express, vol. 26, no. 5, 6114 (2018)

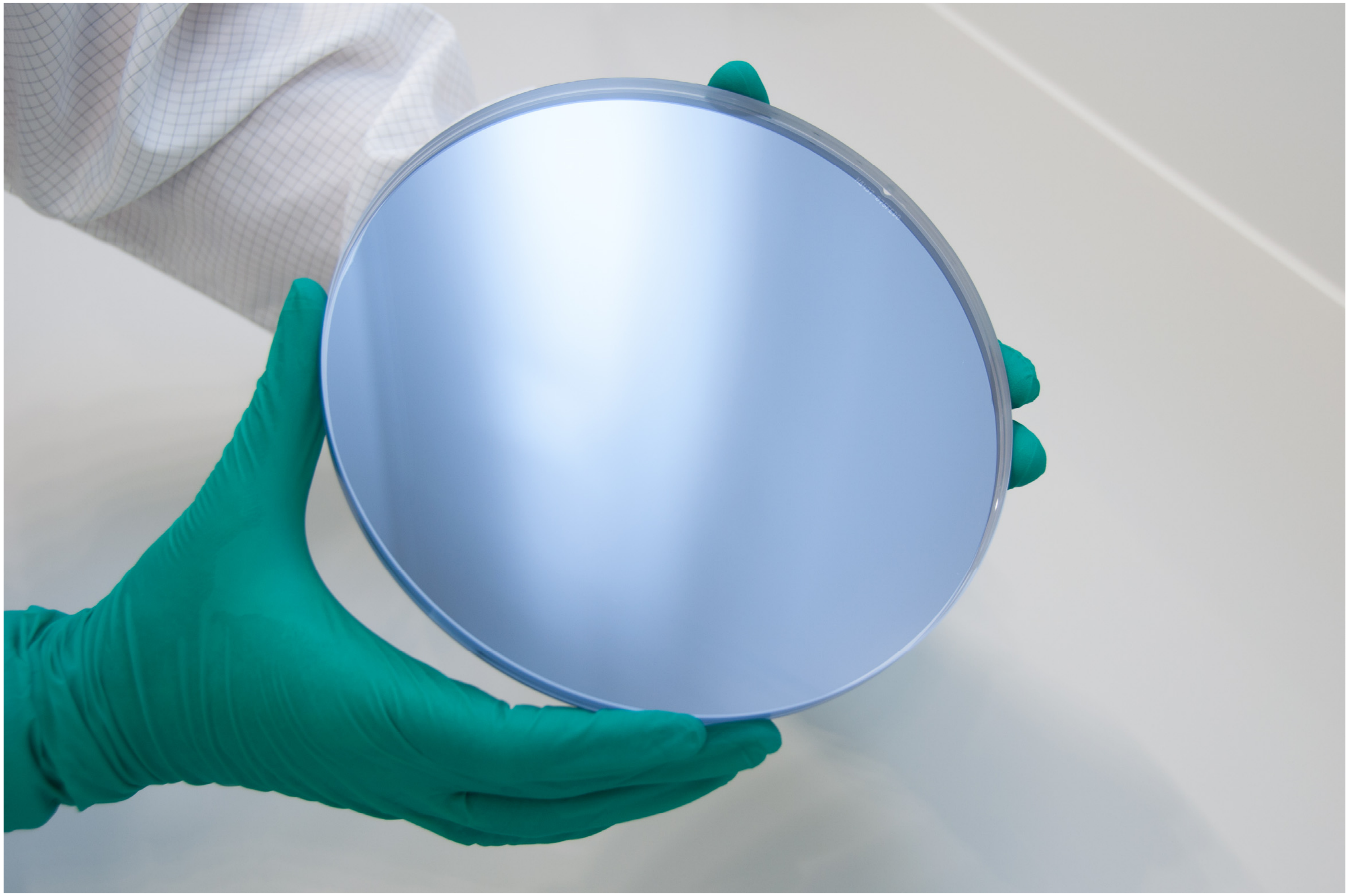

- LIGO-relevant bonding demo: 200-mm diam. GaAs bonded to SiO_2

- Introduction to substrate-transferred crystalline coatings
- Microfabrication-based coating process overview
- **Advantages of bonded single-crystal interference coatings**
  - **low elastic losses and minimal Brownian noise**
  - **mid-infrared optical transparency**
  - **high thermal conductivity**

- Various substrate materials and geometries possible
  - SiO_2, Si, SiC, Al_2O_3, YAG, YVO_4, diamond, etc.
  - ROC > 10 cm
  - 20 cm maximum diameter
- Ultralow Brownian noise
  - loss angle reduced 10-100 ×
- Low mid-IR optical losses
  - < 50 ppm loss to 5 μm
- High thermal conductivity
  - ~30 $Wm^{-1}K^{-1}$ GaAs/AlGaAs
- Respectable LIDT values
  - ~8 J/cm^2 for ns pulses
  - > 50 MW/cm^2 CW

- Various substrate materials and geometries possible
  - SiO_2, Si, SiC, Al_2O_3, YAG, YVO_4, diamond, etc.
  - ROC > 10 cm
  - 20 cm maximum diameter
- Ultralow Brownian noise
  - loss angle reduced 10-100×
- Low mid-IR optical losses
  - < 50 ppm loss to 5 μm
- High thermal conductivity
  - ~30 $Wm^{-1}K^{-1}$ GaAs/AlGaAs
- Respectable LIDT values
  - ~8 J/cm^2 for ns pulses
  - > 50 MW/cm^2 CW

Pound-Drever-Hall Laser Frequency Stabilization System

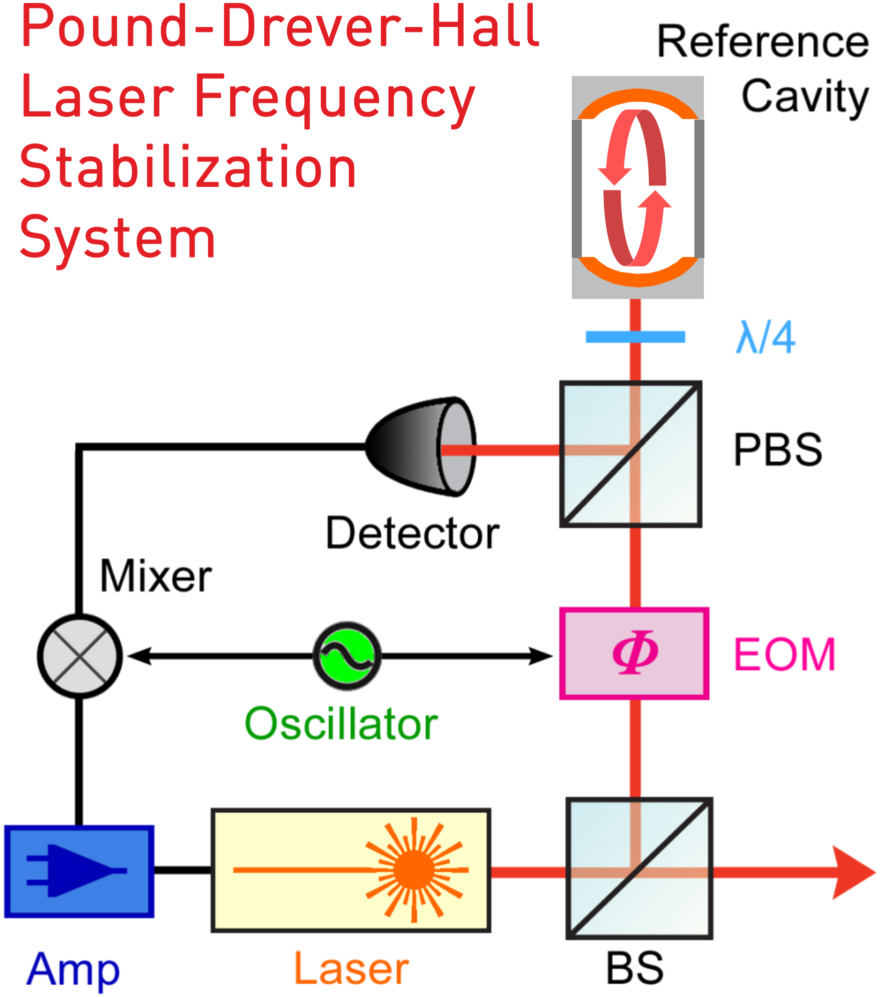

- Stabilized lasers for precision measurement and metrology
  - high-resolution spectroscopy
  - optical atomic clocks
  - frequency dissemination
  - enhanced navigation systems
- Fractional frequency stability:

$$\frac{\Delta f}{f} = -\frac{\Delta L}{L} - \frac{\Delta n}{n} + \delta_{Lock}$$

  - small pressure fluctuations
  - stable, low noise lock loop
  - low temp. & vibration sensitivity
- Strict path length constraints
  - $\Delta f/f \sim 10^{-16} \rightarrow \Delta L \sim 10^{-17}$ m (10 cm)

Pound-Drever-Hall Laser Frequency Stabilization System

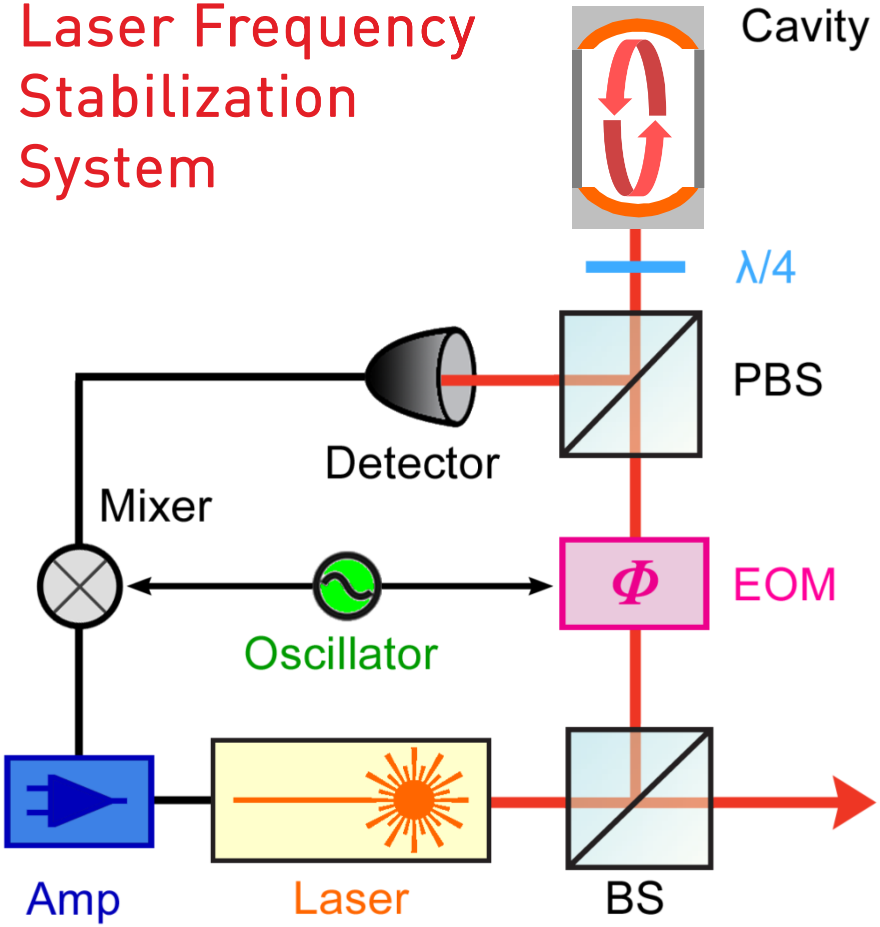

- Stabilized lasers for precision measurement and metrology
  - high-resolution spectroscopy
  - optical atomic clocks
  - frequency dissemination
  - enhanced navigation systems
- Fractional frequency stability:

$$\frac{\Delta f}{f} = -\frac{\Delta L}{L} - \frac{\Delta n}{n} + \delta_{Lock}$$

  - small pressure fluctuations
  - stable, low noise lock loop
  - low temp. & vibration sensitivity
- Strict path length constraints
  - $\Delta f/f \sim 10^{-16} \rightarrow \Delta L \sim 10^{-17}$ m (10 cm)

Pound-Drever-Hall Laser Frequency Stabilization System

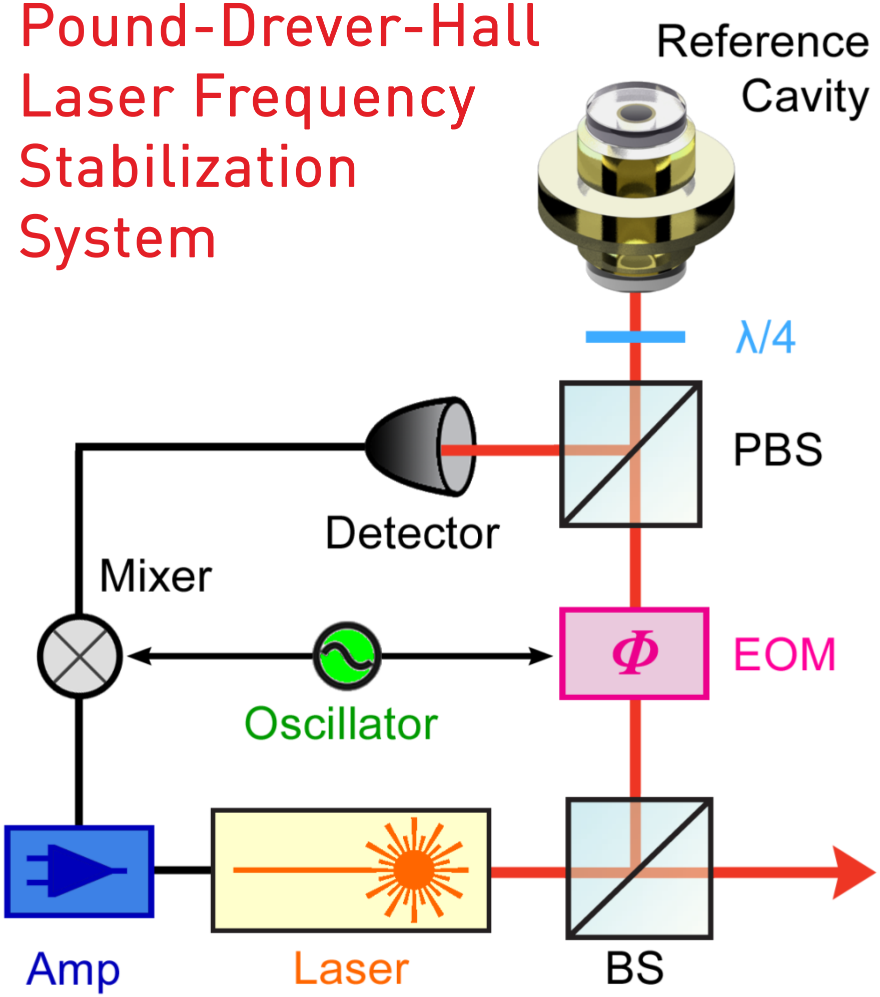

- Stabilized lasers for precision measurement and metrology
  - high-resolution spectroscopy
  - optical atomic clocks
  - frequency dissemination
  - enhanced navigation systems
- Fractional frequency stability:

$$\frac{\Delta f}{f} = -\frac{\Delta L}{L} - \frac{\Delta n}{n} + \delta_{Lock}$$

  - small pressure fluctuations
  - stable, low noise lock loop
  - low temp. & vibration sensitivity
- Strict path length constraints
  - $\Delta f/f \sim 10^{-16} \rightarrow \Delta L \sim 10^{-17}$ m (10 cm)

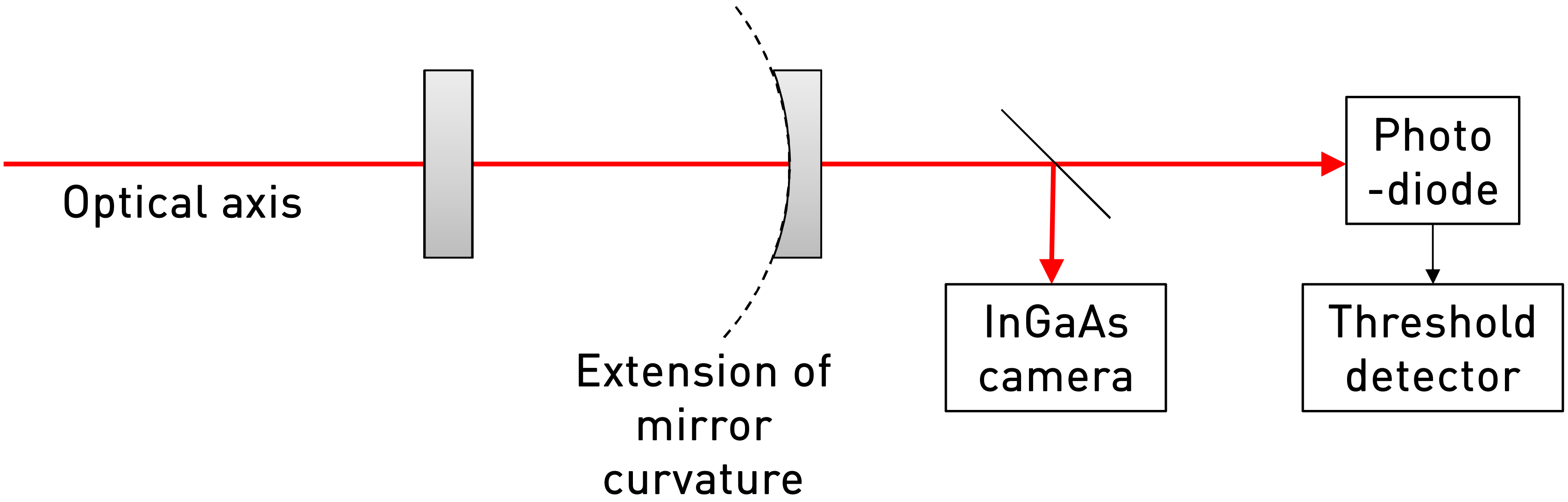

- Cavity mirrors are held in 4-DOF mounts: translation and tip-tilt
  - the surface normal of a spherical mirror can be re-aligned to the cavity mode after a transverse displacement by applying a rotation
- Cavity mode is rastered across surface of mirror under test
- After each translation, automated transverse cavity mode detection adjusts the rotation of the mirror to excite the fundamental mode

Truong et al., Optics Express, vol. 27, no. 14, 19141 (2019)

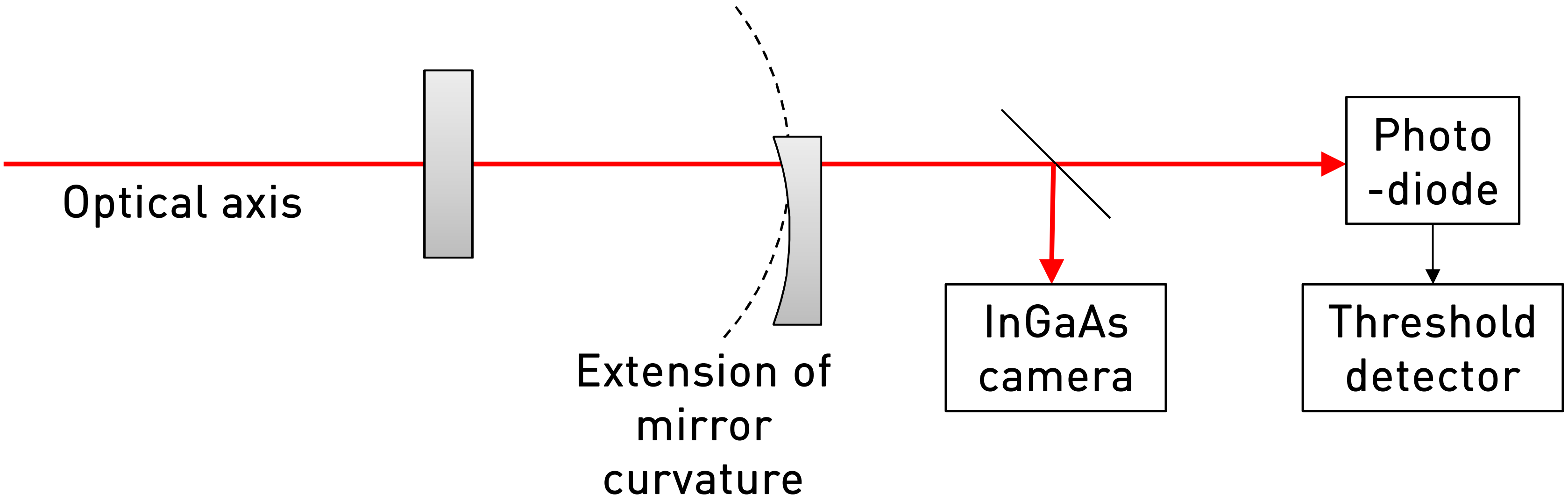

- Cavity mirrors are held in 4-DOF mounts: translation and tip-tilt
    - the surface normal of a spherical mirror can be re-aligned to the cavity mode after a transverse displacement by applying a rotation
- Cavity mode is rastered across surface of mirror under test
- After each translation, automated transverse cavity mode detection adjusts the rotation of the mirror to excite the fundamental mode

Truong et al., Optics Express, vol. 27, no. 14, 19141 (2019)

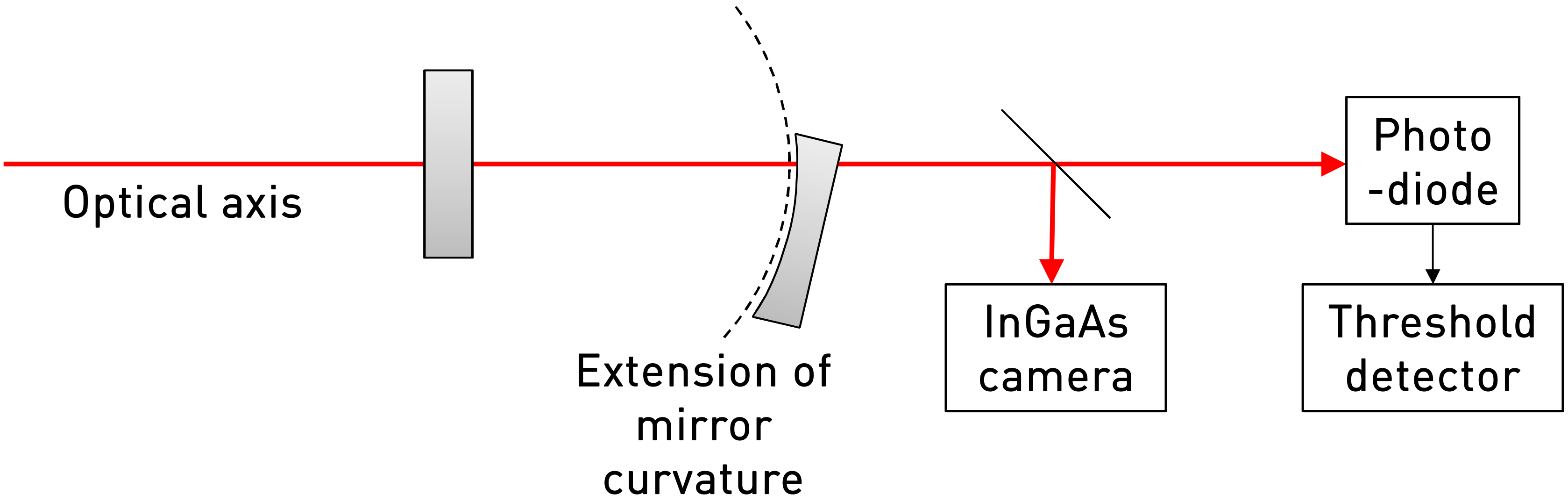

- Cavity mirrors are held in 4-DOF mounts: translation and tip-tilt
  - the surface normal of a spherical mirror can be re-aligned to the cavity mode after a transverse displacement by applying a rotation
- Cavity mode is rastered across surface of mirror under test
- After each translation, automated transverse cavity mode detection adjusts the rotation of the mirror to excite the fundamental mode

Truong et al., Optics Express, vol. 27, no. 14, 19141 (2019)

Spatially-Resolved Cavity Ringdown

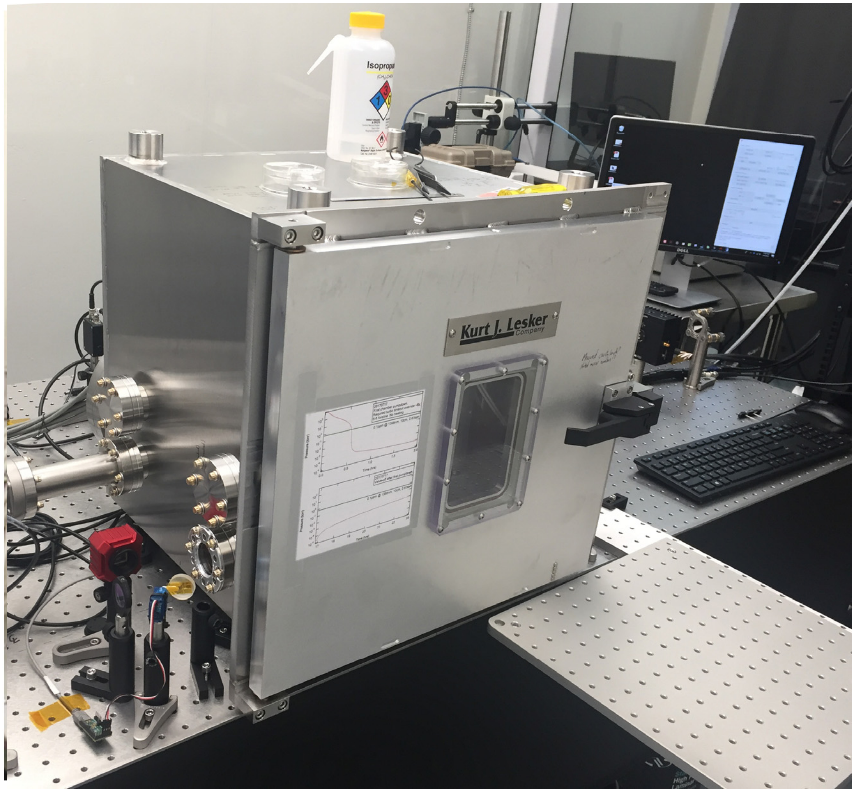

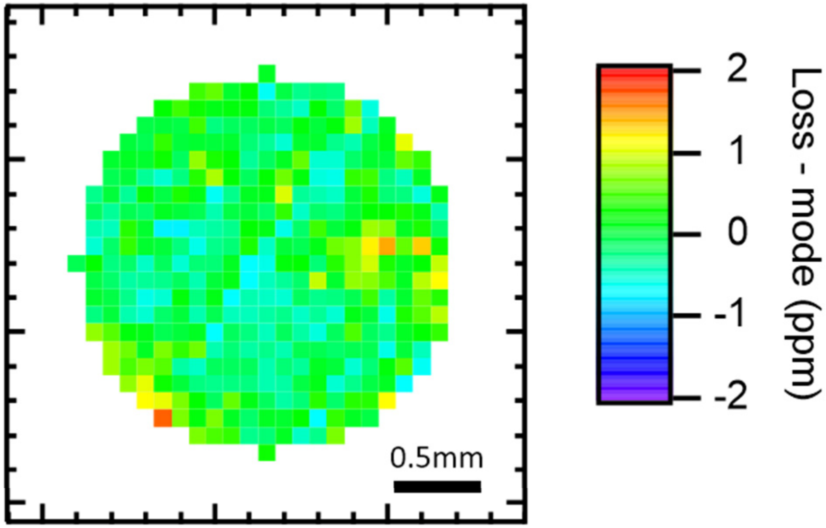

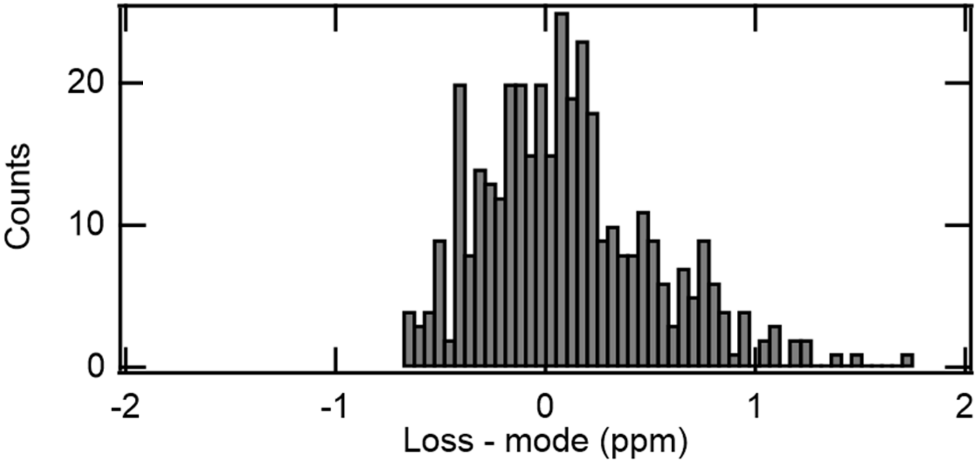

T = 9 ppm, mode = 16.7 ppm

- Encoded motors offer a few-μm accuracy and < 1 μm precision
- Accommodates 2-in diam. substrates
- Automated scans up to 8×8 mm^2 at 0.1 mm pitch demonstrated
- Wavelengths: 1064, 1156, 1397, 1550 nm

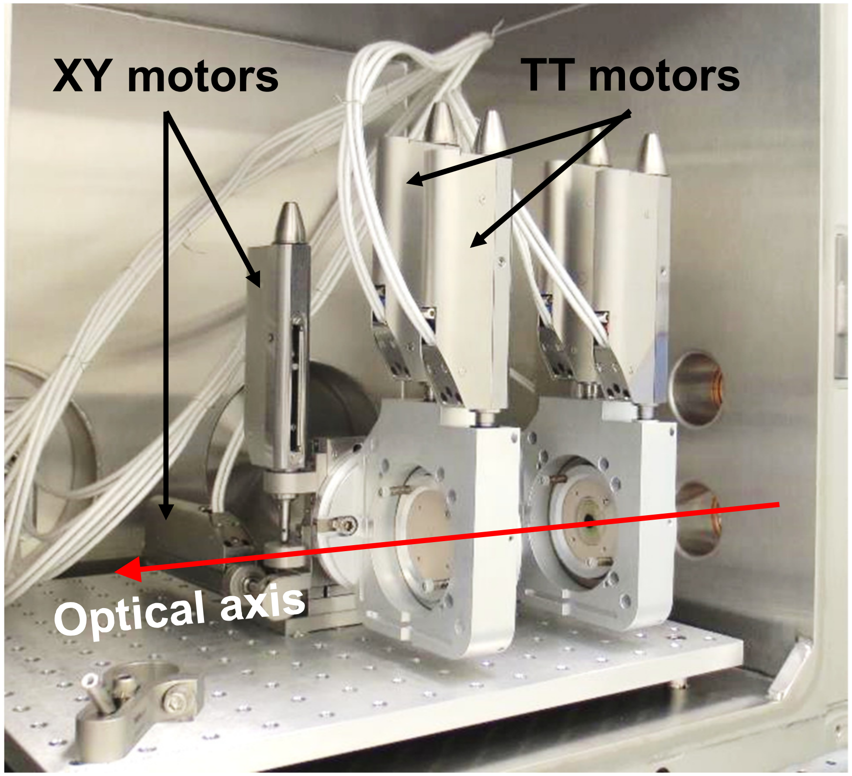

- Encoded motors offer a few-μm accuracy and < 1 μm precision
- Accommodates 2-in diam. substrates
- Automated scans up to 8×8 mm^2 at 0.1 mm pitch demonstrated
- Wavelengths: 1064, 1156, 1397, 1550 nm

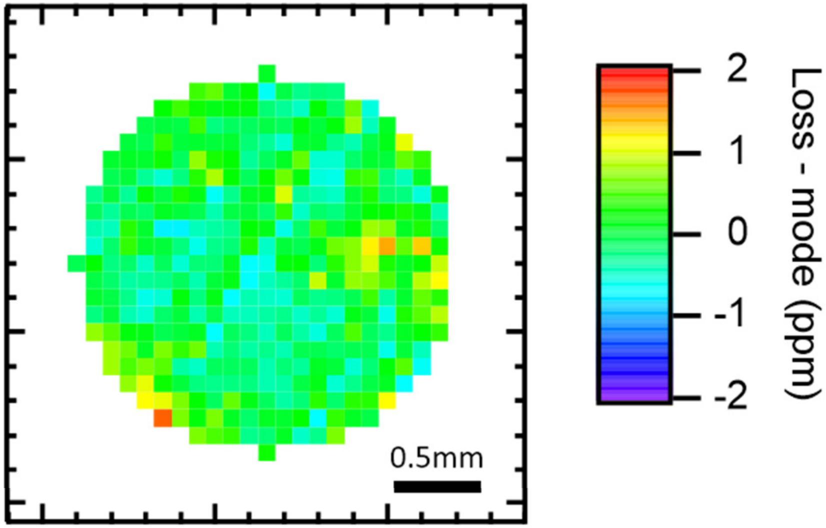

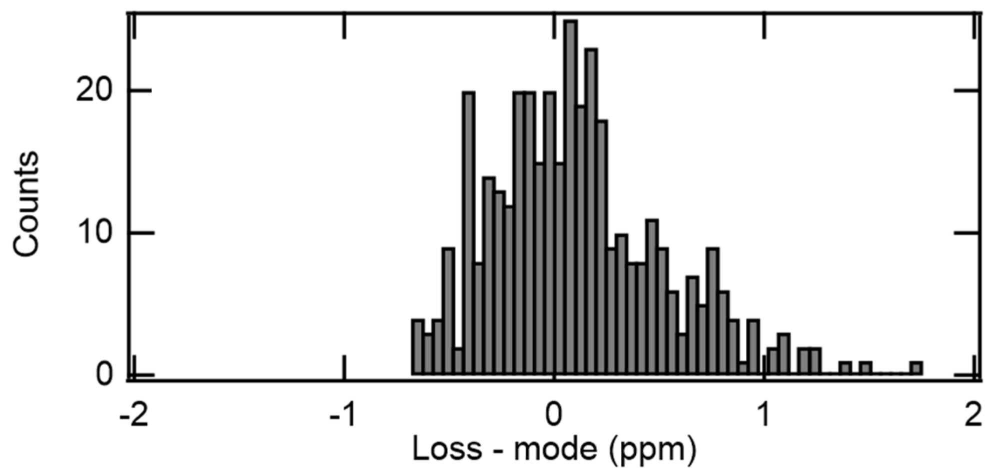

T = 9 ppm, mode = 16.7 ppm

Custom Optical Reference Cavities and Low-Noise Optics

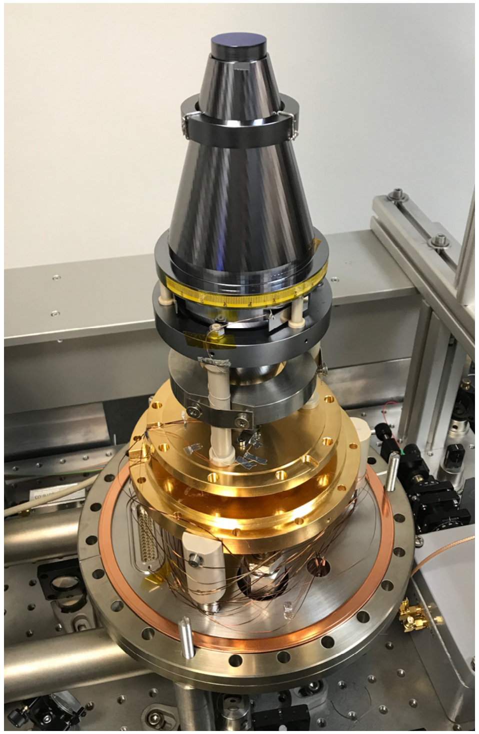

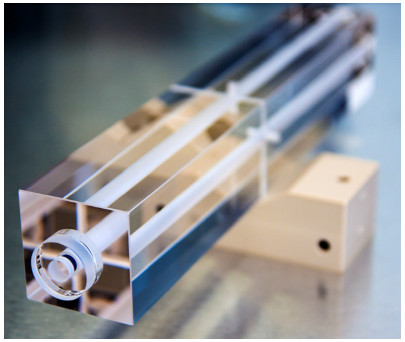
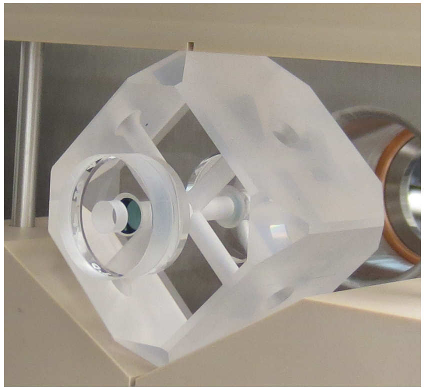
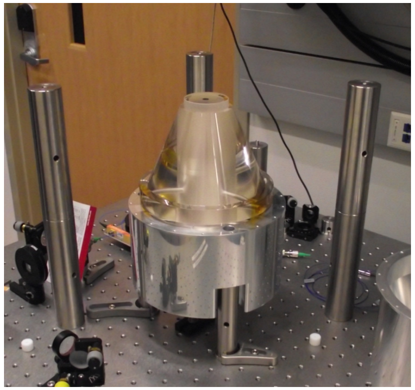

- Dozens of cavities & mirrors deployed on SiO_2, Si, and Al_2O_3 subs.
- Mirror diameters of 0.5" to 2" and spacer lengths up to 30 cm
- Wavelengths from ~1000 nm to 1600 nm, RT and cryo (4-124 K)
  - excess losses < 3 ppm measured via ringdown, reflectivity > 99.999%

Custom Optical Reference Cavities and Low-Noise Optics

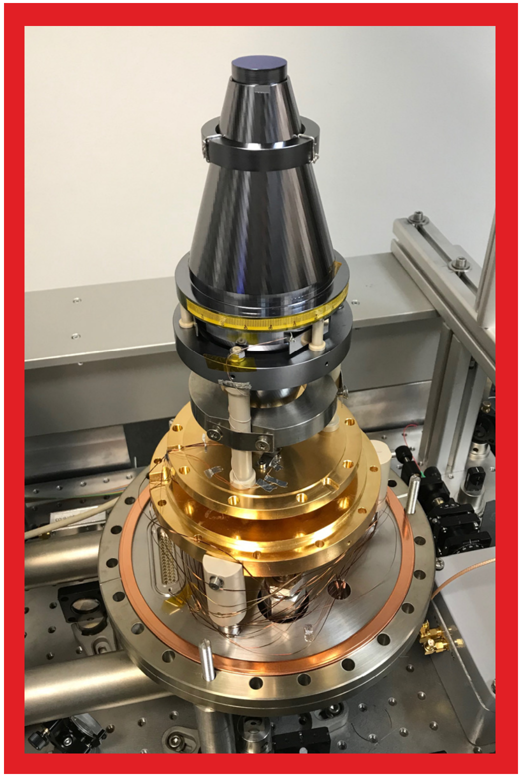

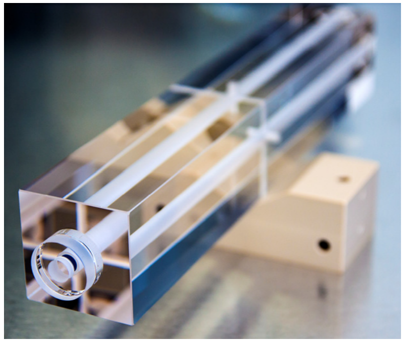

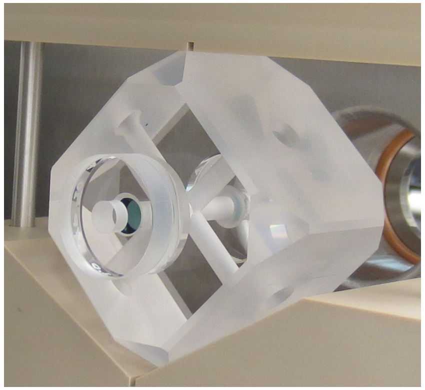

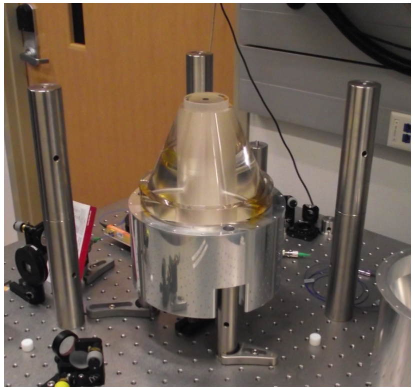

- Dozens of cavities & mirrors deployed on SiO_2, Si, and Al_2O_3 subs.
- Mirror diameters of 0.5” to 2” and spacer lengths up to 30 cm
- Wavelengths from ~1000 nm to 1600 nm, RT and cryo (4-124 K)
    - excess losses < 3 ppm measured via ringdown, reflectivity > 99.999%

- Various substrate materials and geometries possible
  - SiO_2, Si, SiC, Al_2O_3, YAG, YVO_4, diamond, etc.
  - ROC > 10 cm
  - 20 cm maximum diameter
- Ultralow Brownian noise
  - loss angle reduced 10-100 ×
- Low mid-IR optical losses
  - < 50 ppm loss to 5 µm
- High thermal conductivity
  - ~30 $Wm^{-1}K^{-1}$ GaAs/AlGaAs
- Respectable LIDT values
  - ~8 J/cm^2 for ns pulses
  - > 50 MW/cm^2 CW

Spectroscopy in the Mid-Infrared

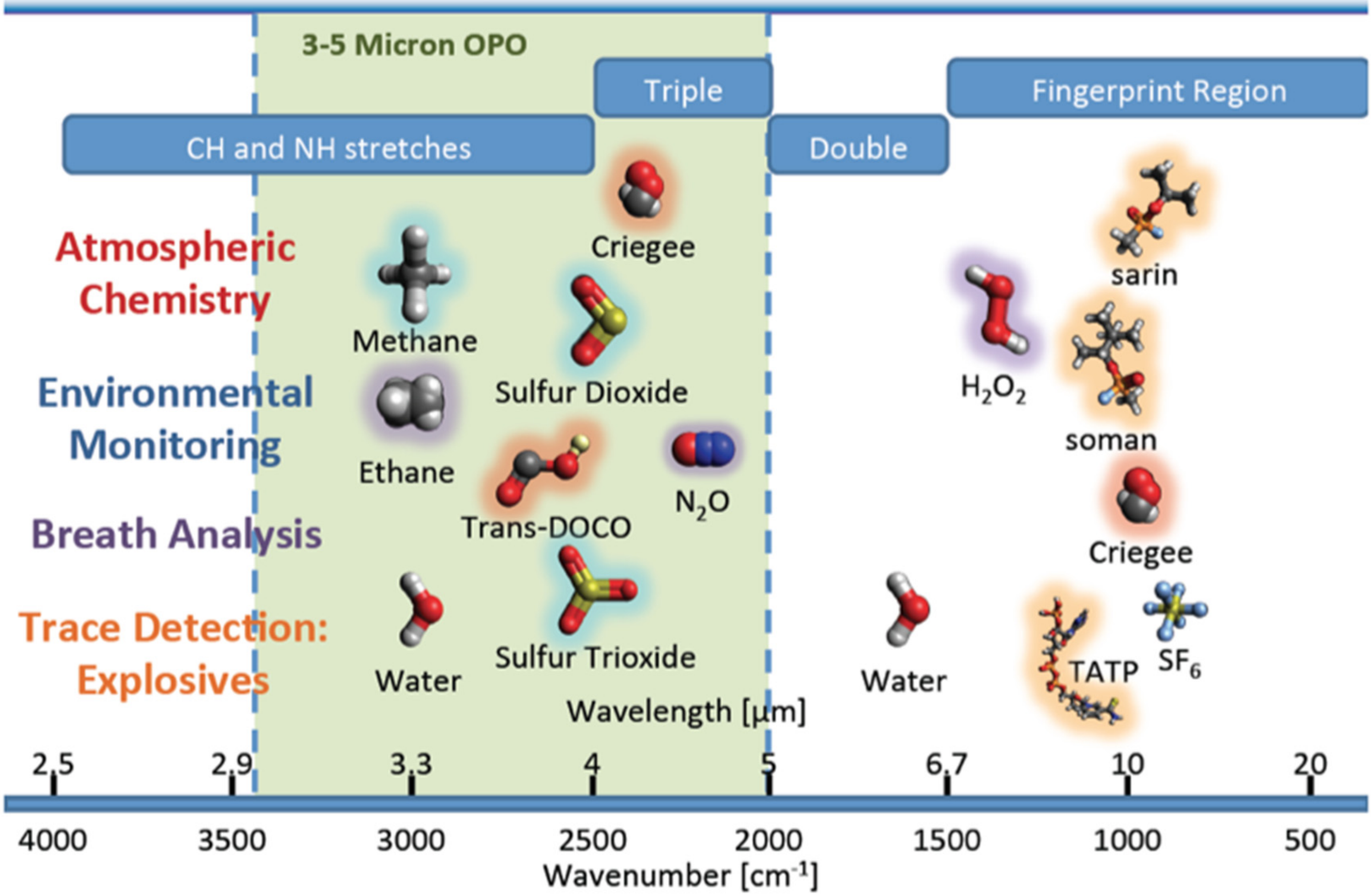

Mid-Infrared Spectroscopy

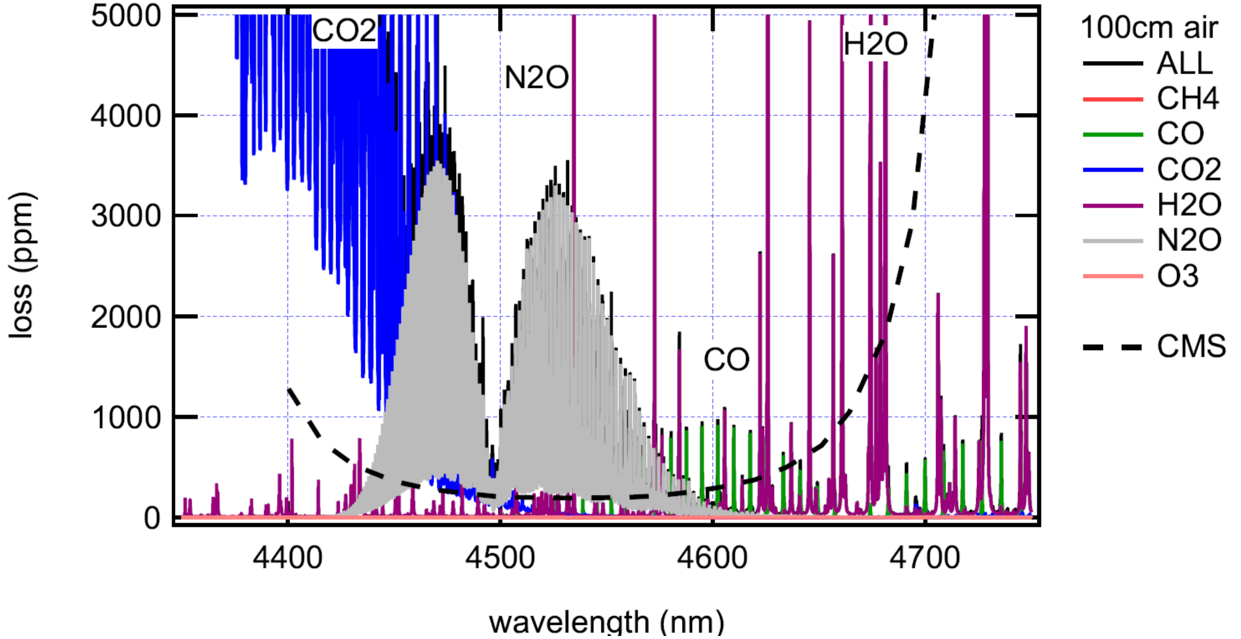

- Cavity ring-down optics in the MIR lag behind their NIR counterparts
  - evaporated coatings show large variation in losses, typically > 100 ppm
  - there is a need for mirrors w/ enhanced repeatability and robustness
- We have fabricated prototype mirrors from 3.3 to 4.6 μm targeting methane sensing, atmospheric chem., and C isotope identification

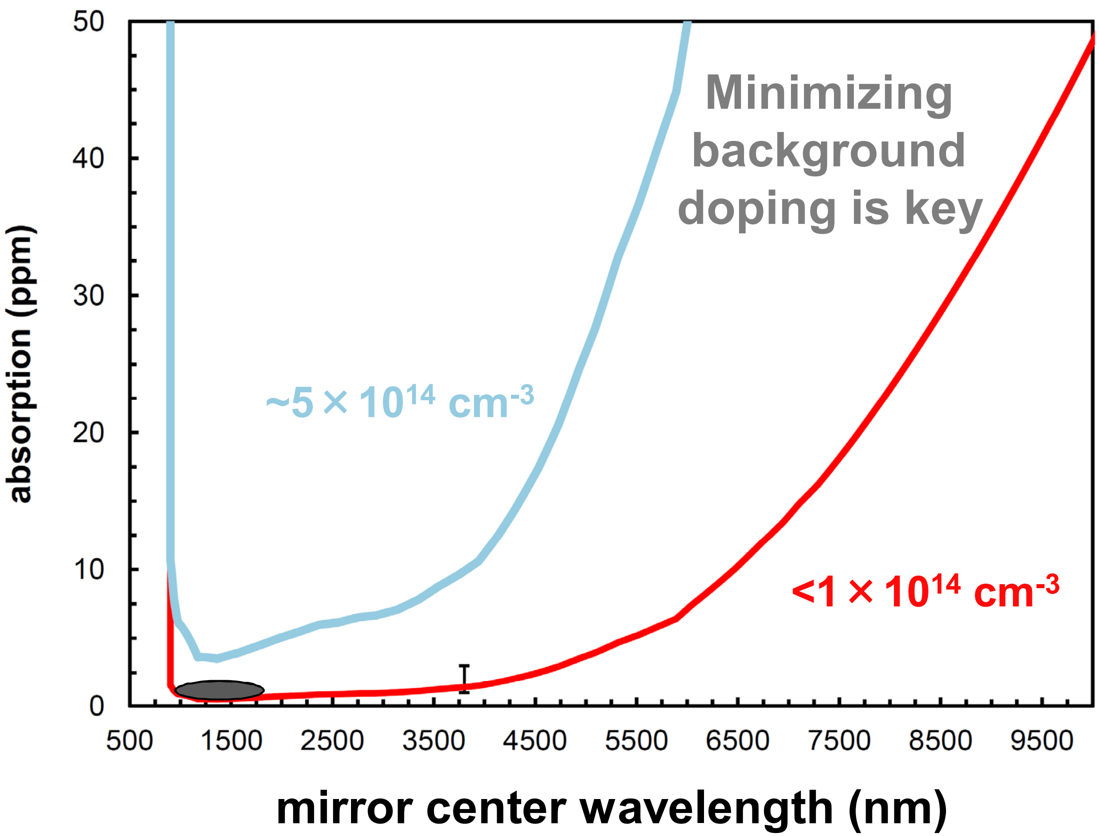

- Plot incorporates
  - material dispersion
  - absorption coefficient
  - penetration depth
- Assumes n-type background doping
- GaAs band-edge limits operation to >900 nm
  - short-wave cutoff
- Absorption increases rapidly beyond 5 μm
  - free-carrier absorption
  - proportional to λ^3

For abs. coeff. see: W. G. Spitzer and J. M. Whelan, Physical Review 114, April 1959

Prototype Mid-IR Crystalline Coatings

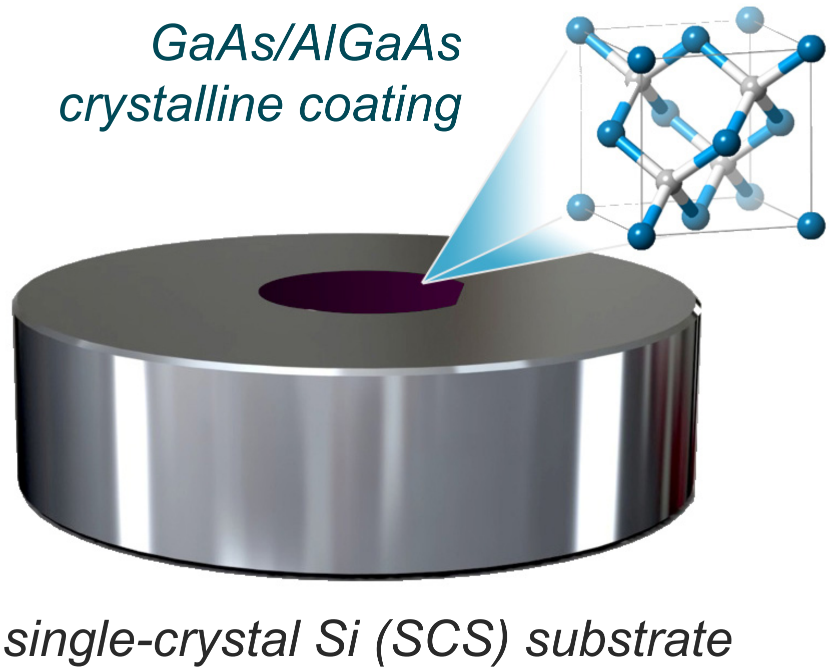

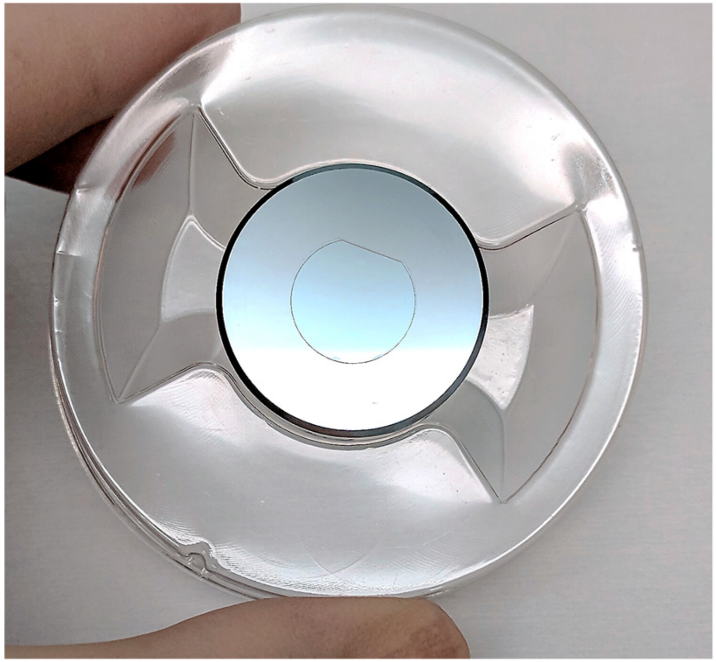

- Monocrystalline mirror discs transferred to curved SCS substrates
  - based on an extension of our cryogenic Si cavity end mirrors
  - potential for optical losses below at or below 20 ppm to ~5 or 6 µm

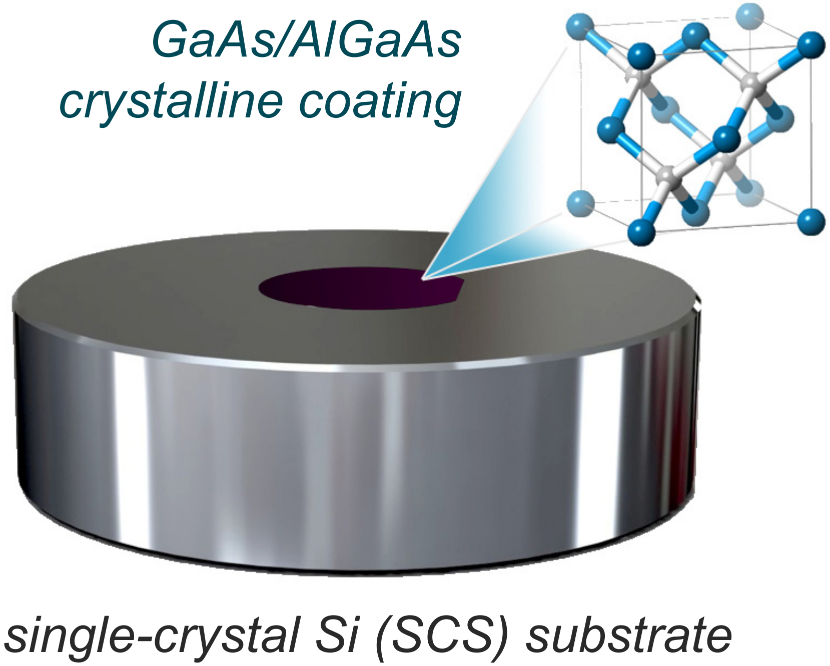

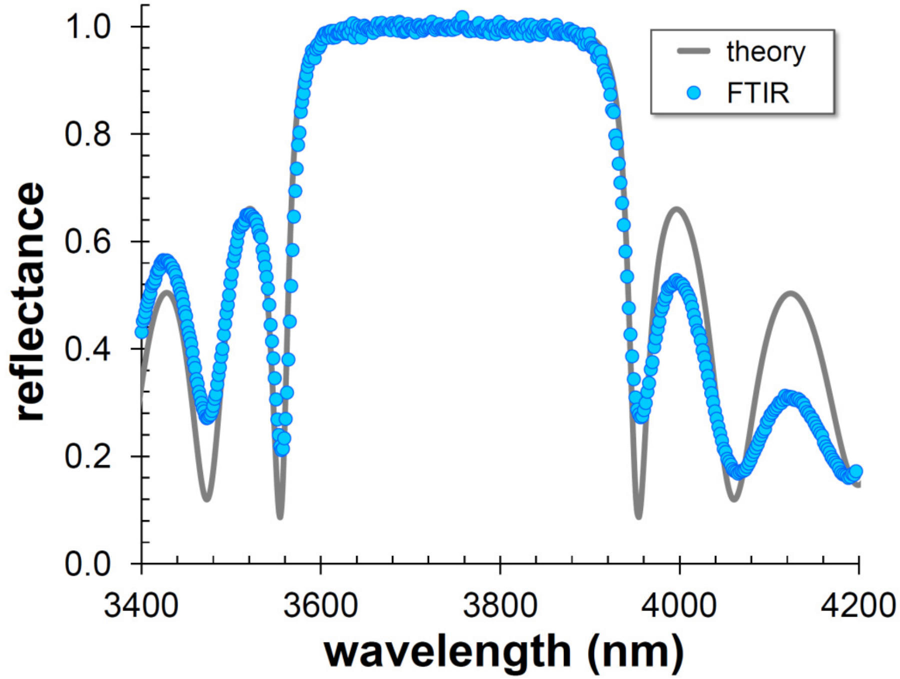

- Monocrystalline mirror discs transferred to curved SCS substrates
  - based on an extension of our cryogenic Si cavity end mirrors
  - potential for optical losses below at or below 20 ppm to ~5 or 6 μm

O_3 —*266 nm photolysis*→ O_2 + O (^{1}D)

O (^{1}D) + D_2 → OD + D

OD + CO → **DOCO**

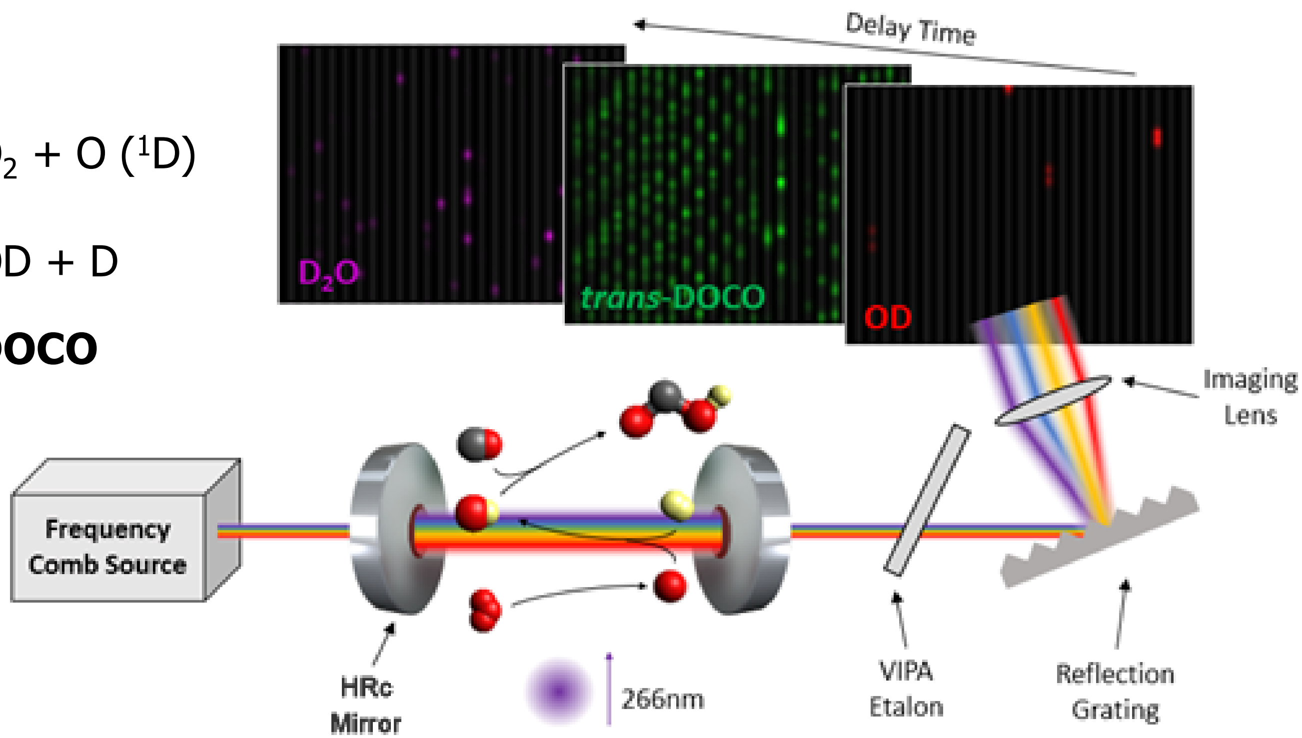

- First observation of trans-DOCO realized with CMS's 3.7 µm mirrors
- Reaction rates for the formation of DOCO
  - important for CO_2 / CO abundance in atmosphere
  - heat release mechanism in combustion processes

B.J. Bjork, et al., Science 354, 444 (2016)

Total Loss Measurements Result

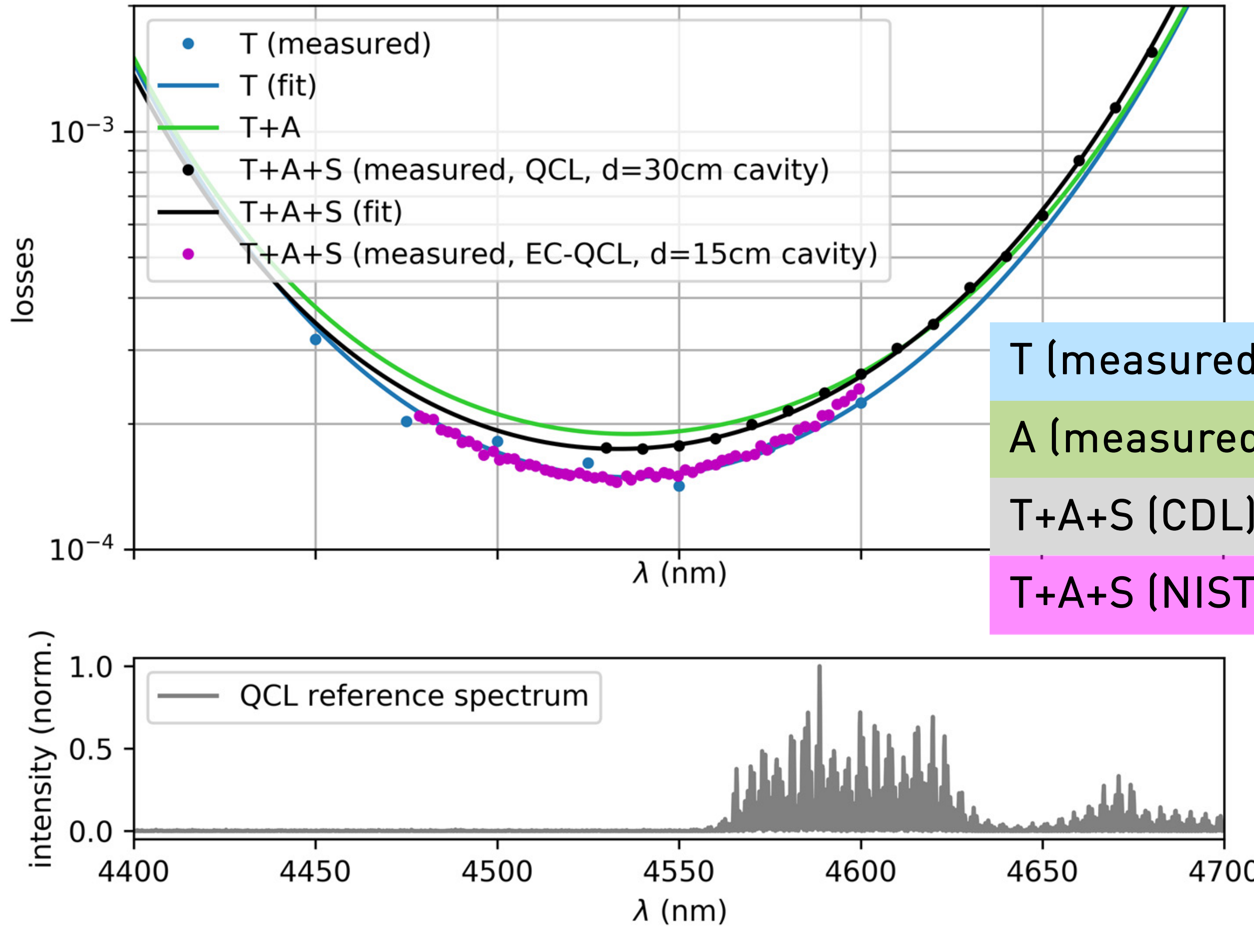

	Loss (ppm)	λ_{min} (nm)
T (measured)	144±10	4531±10
A (measured)	40±10	4550-4700
T+A+S (CDL)	175±5	4536±10
T+A+S (NIST)	149±1.5	~4530

- Slight discrepancy between CDL and NIST data (L = 175 / 150 ppm resp.)
  - likely driven by difference in cavity length and thus spot size
- Direct absorption and trans. to be re-examined, currently 16 < A < 46 ppm

Orientation-Dependent Absorption

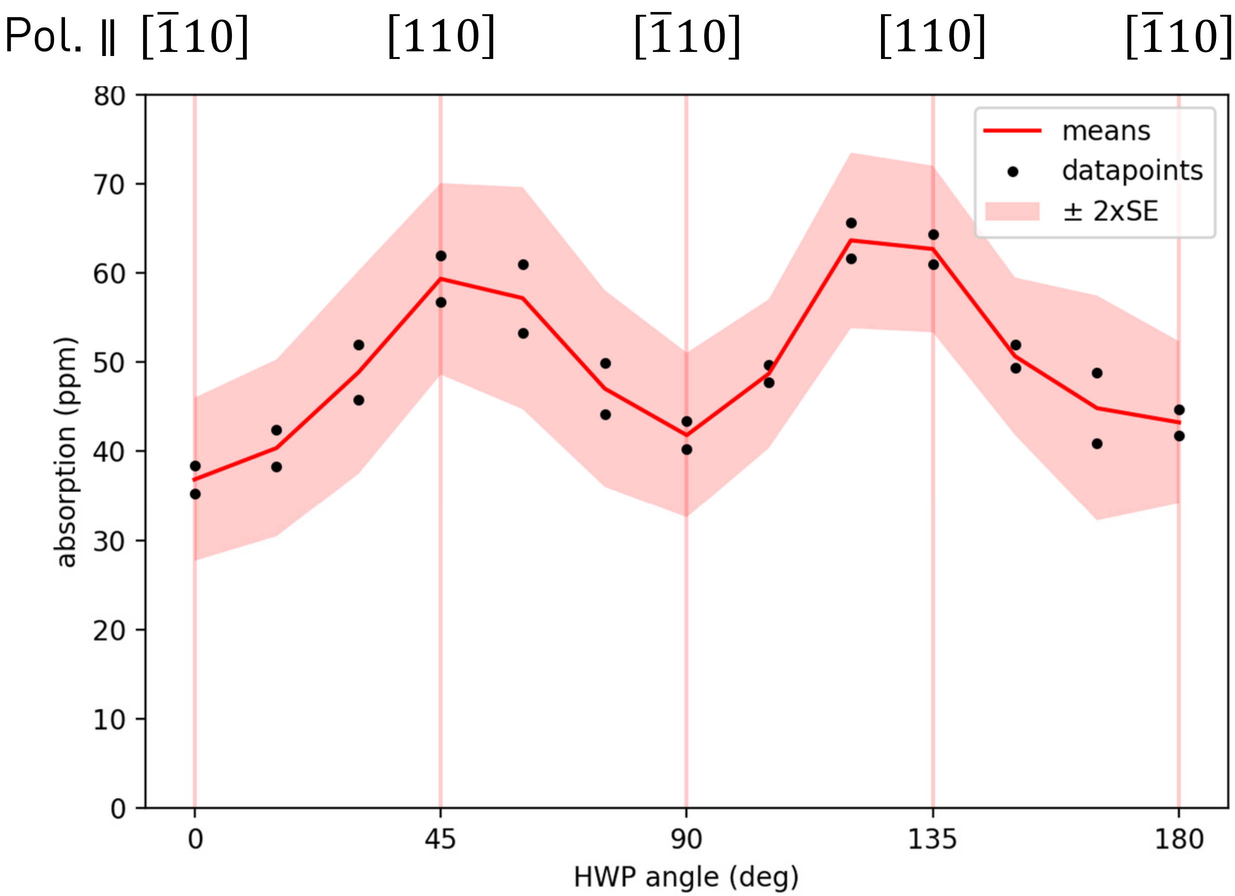

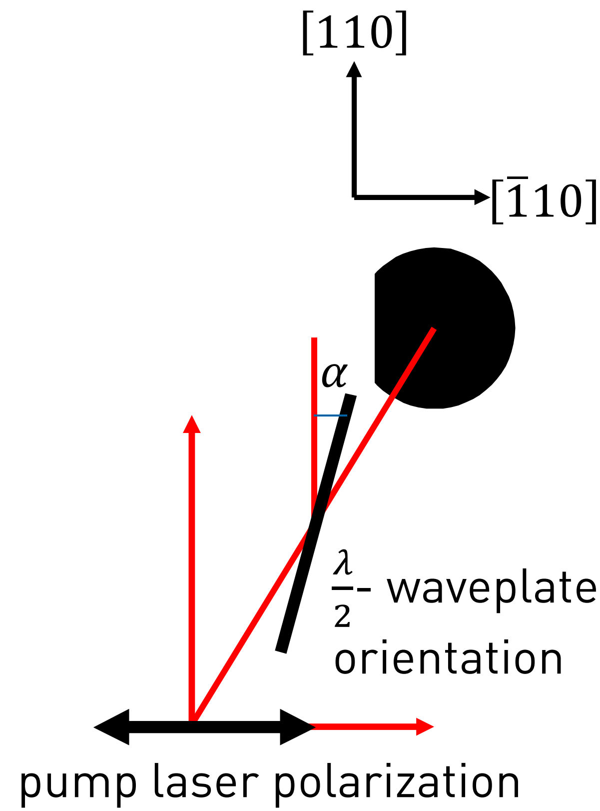

- Orientation-dependent absorption observed for linear polarization
- Investigations underway to determine the underlying cause
  - intrinsic or strain induced variation in band structure

- Various substrate materials and geometries possible
  - SiO_2, Si, SiC, Al_2O_3, YAG, YVO_4, diamond, etc.
  - ROC > 10 cm
  - 20 cm maximum diameter
- Ultralow Brownian noise
  - loss angle reduced 10-100 ×
- Low mid-IR optical losses
  - < 50 ppm loss to 5 μm
- High thermal conductivity
  - ~30 $Wm^{-1}K^{-1}$ GaAs/AlGaAs
- Respectable LIDT values
  - ~8 J/cm^2 for ns pulses
  - > 50 MW/cm^2 CW

Superior Thermal Conductivity

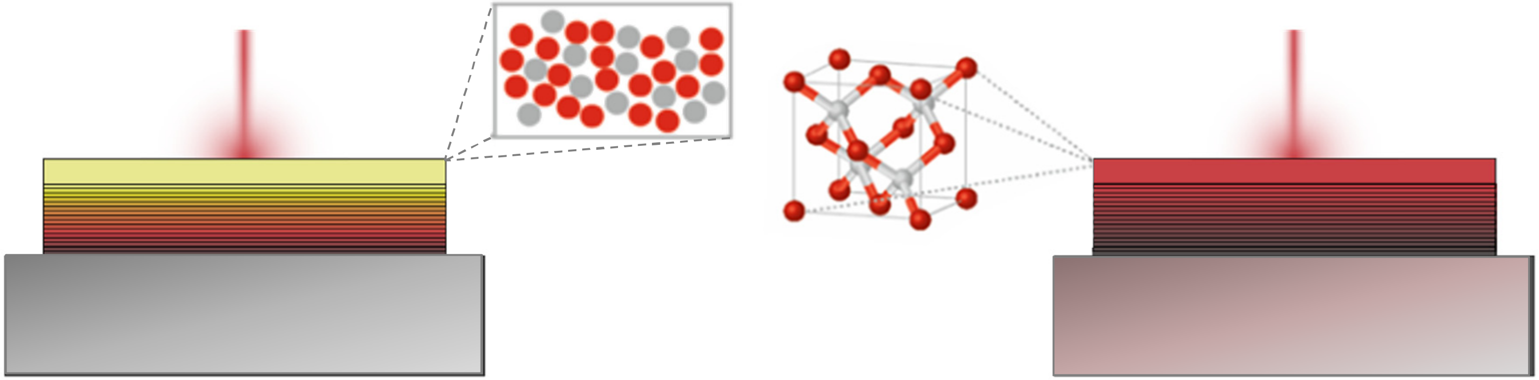

SiO_2/Ta_2O_5
Amorphous
$\kappa \approx 1\ Wm^{-1}K^{-1}$

GaAs/AlGaAs
Single Crystal
$\kappa \approx 30\ Wm^{-1}K^{-1}$

- Thermal conductivity ~30 × greater than standard mirror coatings
  - potential for reduced thermal lensing, wavefront distortion, etc.
- Novel applications in high power laser machining systems
  - high thermal conductivity in combination with ultralow optical losses
  - CW laser-induced damage threshold measured to be >50 MW/cm^2

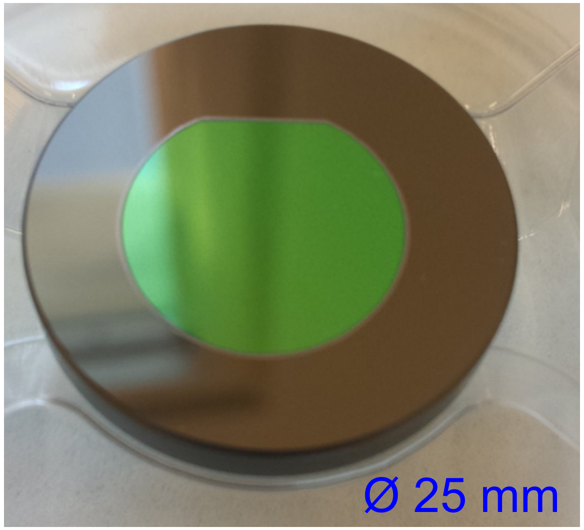

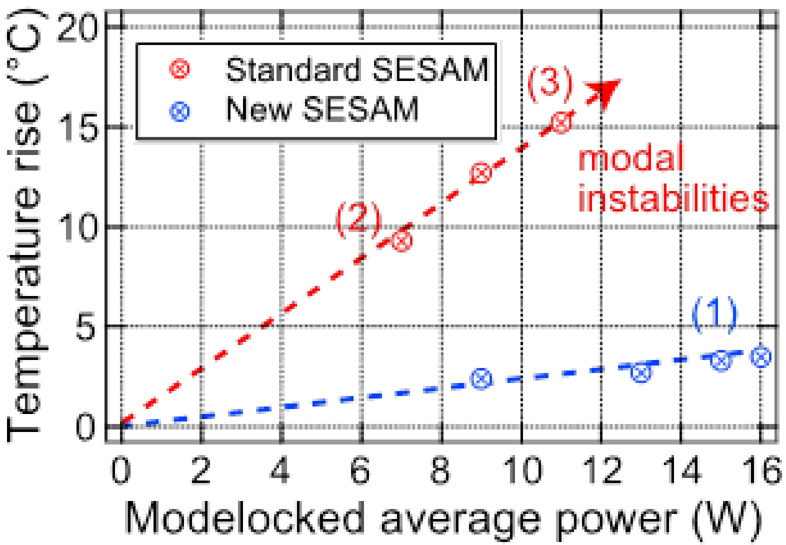

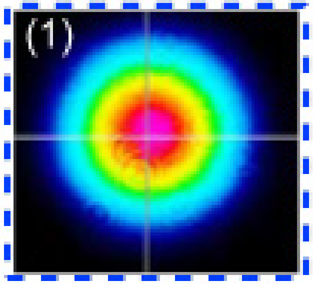

- GaAs-based saturable absorber mirror (SESAMs) transferred to SiC
  - large area coating with superior flatness and enhanced heat transfer
- Structure enables power scaling by avoiding modal instabilities
  - demonstrated for peak powers up to 10 MW, goal is to push to 100 MW
- Similar application: laser active media bonded to diamond

in collaboration with Ursula Keller (ETH) and Thomas Südmeyer (Neuchatel)

Direct-bonded Yb:YAG on SiC

Yb:YAG disk on SiC

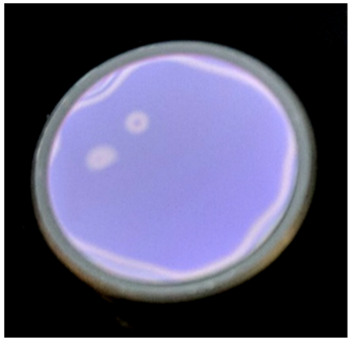

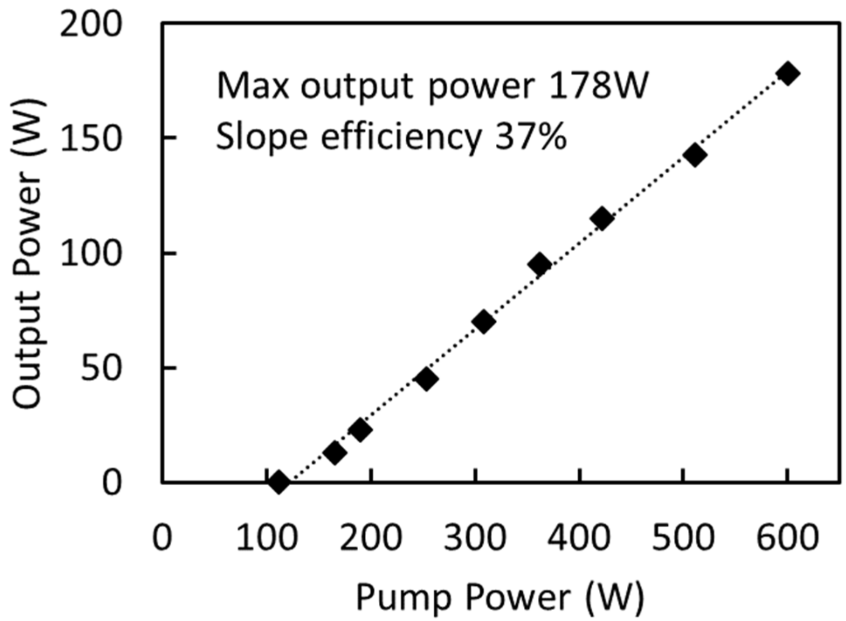

Output beam profile

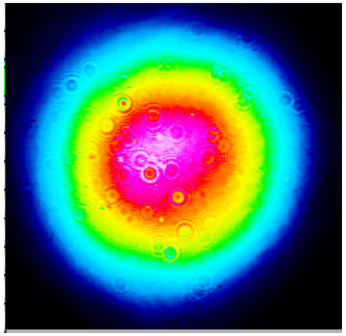

- Pumped with 4 mm diameter spot and maximum power of 600 W
- 178 W single-mode output at 1030 nm
- M^2 of 1.02 (M^2x) and 1.10 (M^2y)
- Direct bonding achieves very low thermal resistivity
- Dual benefit would come with the crystalline coatings

in collaboration with L. Deyra (ALPhANOV)

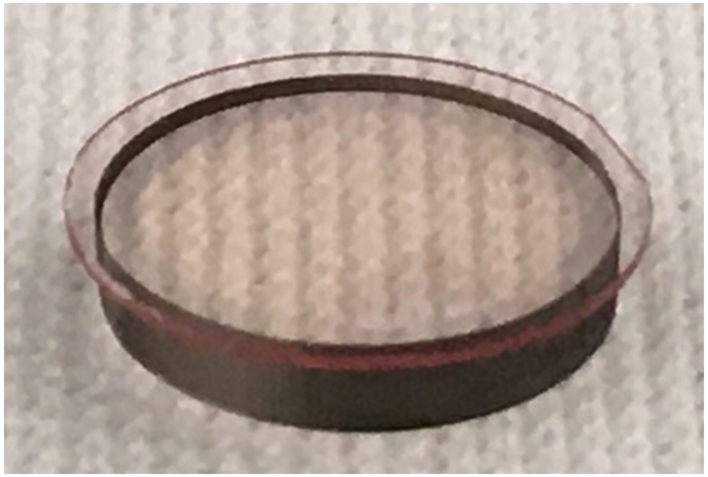

Ti:sapph / single-crystal diamond

Diamond-clad Ti:sapph

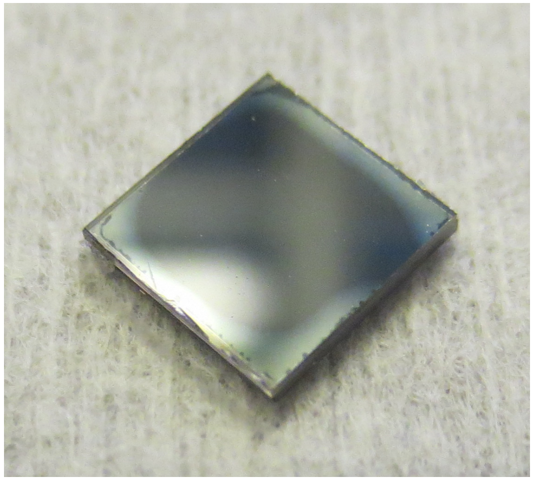

SiC-clad InGaAs/GaAs

- With sufficient surface quality, direct bonding is possible
  - RMS microroughness <1 nm, surface figure at λ/10 or better
  - local ROC >10 cm, no defects > 50 μm in size
- With proper surface treatment bulk bond strength is possible
  - typical Van der Waals strength of 70 mJ/m^2, fusion bonding: 1 J/m^2

Substrate-transferred crystalline coatings simultaneously exhibit excellent optical and thermo-mechanical quality

- Elastic loss reduction of 10-100 × compared w/ IBS films
  - IBS-deposited Ta_2O_5/SiO_2: typical Q ~3000 ($\varphi_{IBS} \approx 2\text{-}4 \times 10^{-4}$)
  - AlGaAs Q-values from 4×10^4 ($\varphi_{RT} \approx 2 \times 10^{-5}$)
  - AlGaAs cryogenic performance: Q $>1 \times 10^5$ ($\varphi_{min} \approx 4.5 \times 10^{-6}$)
- Minimal scattering loss and optical absorption
  - absorption verified at <1 ppm, scatter loss <5 ppm
  - measured finesse $>2 \times 10^5$ at 1064, 1156, 1397, and 1550 nm
- Potential for ppm-level optical losses in the MIR
  - optical absorption <50 ppm for wavelengths out to 4.6 µm
- Reasonably high multilayer thermal conductivity
  - in-plane value of 55-85 $Wm^{-1}K^{-1}$ through thickness ~30 $Wm^{-1}K^{-1}$


Thank you for your attention!
CMS
CRYSTALLINE MIRROR SOLUTIONS